AGSO Journal of Australian Geology & Geophysics, 16 (4), 399–420

The signature of terrestrial impacts

Richard A.F. Grieve[1] & Mark Pilkington[1]

The high level of endogenic geological activity makes the terrestrial record of impact difficult to read. Terrestrial processes, such as erosion, rapidly modify craterforms and ultimately remove the evidence of impact. In their largely uneroded states, terrestrial impact structures have the basic so-called simple and complex forms observed on other planetary bodies, but few of them have morphometric parameters, such as apparent and true depth and stratigraphic uplift, that can be defined. Erosion severely affects such parameters, and can even result in a positive topographic form due to differential erosion. The principal criterion for the recognition of terrestrial impact structures is, therefore, not their form, but the occurrence of shock-metamorphic effects. These are well-documented and are described briefly. In parautochthonous target lithologies, they are limited to the central portion of the original crater floor, and attenuate radially and with depth. Shock effects also occur in allochthonous lithologies, such as breccias and impact-melt rocks.

In addition to a characteristic geological signature, terrestrial impact structures have characteristic geophysical signatures. The most common is a Bouguer gravity low, which extends out to the rim. The low is due to impact-induced brecciation and fracturing. It increases in value with increasing size, reaching a limiting value of ~300 μm s^{-2} (~300 g.u.). In large impact structures, it can be accompanied by a central relative high. The magnetic signature can be more varied but generally corresponds to a subdued low. Local intense magnetic anomalies can occur in the centres of large structures, D >40 km; these magnetic highs have various sources, but many are due to post-impact hydrothermal alteration. Impact can also lead to a reduction in seismic velocities and resistivity of the target rocks.

The geophysical, geological, and morphological characteristics at terrestrial impact structures are summarised in tabular form as an aid to the recognition of additional structures.

Introduction

During the last 25 years, our perspective of the planetary bodies of the solar system has changed from them being astronomical to geological objects. With volcanism and, to a lesser extent, tectonism, impact cratering is now recognised as a ubiquitous geological process affecting all the terrestrial planets. Its apparent importance relative to other geological processes is inversely proportional to planetary size. Smaller planetary bodies are less efficient at retaining their internal heat, and are thus less endogenically active over geological time than larger planetary bodies. Thus, they tend to preserve greater portions of their earliest crust. It is this crust that bears overwhelming evidence of the importance of impact, as it dates back to early times in planetary history when the impact flux was greater than two orders of magnitude higher than the present day (Hartmann 1995).

The Earth is the most endogenically active of the terrestrial planets, and thus has retained the poorest sample of the results of impacts which have occurred throughout geological time. The study of terrestrial impact structures does not have a long established tradition in the Earth sciences. In addition, it has, until recently, largely been the provenance of a small number of workers with strong ties to planetary geology. Although the known sample of terrestrial impact structures is small, terrestrial impact structures are the major source of ground-truth data on the geological and geophysical effects of hypervelocity impact at a variety of scales.

Recently, there has been a growing awareness in the more general Earth-science community as to the potential importance of impact for the terrestrial environment. This has been spurred by several recent realisations. They include: the discovery of chemical and physical evidence for the involvement of impact at the Cretaceous–Tertiary (KT) boundary and the associated mass extinction event (e.g., Alvarez et al. 1980; Smit & Hertogen 1980; Bohor et al. 1984) and their relation to the Chicxulub impact structure in the Yucatan Peninsula, Mexico (Table 1; Hildebrand et al. 1991); the resource potential of impact structures, some of which are related to world-class ore deposits, both spatially and genetically (Grieve & Masaitis 1994); and the disastrous consequences of impacts for human civilisation (Gehrels 1994). The detailed study of impact processes, however, is so recent that it is not yet part of the general knowledge base.

Impact involves the transfer of considerable energies to a spatially limited area of the Earth's surface in a very short time interval. As a consequence, local geology of the target area is only of secondary importance, and the geological and geophysical effects of impact are, to a first order, largely independent of the target. The effects are, however, scale-dependent on the size of the impact. The net result is that, at least before they are modified by post-impact endogenic processes, impacts of similar scale produce similar first-order results. Thus, even though the number of known terrestrial impact structures is small (~150; Grieve et al. 1995), we can derive some general observations with respect to their appearance and geological and geophysical signatures. This contribution outlines some of these observations. We hope that it permits known structures to be placed in context, and provides a guide to the recognition of features consistent with an impact origin at additional structures.

General appearance of terrestrial impact structures

Morphology

Impact structures on other planetary bodies are recognised by their characteristic forms. The morphology of impact structures is divided into simple and complex structures (Dence 1968). Simple structures have the form of a bowl-shaped depression with a structurally uplifted rim, which includes an overturned flap overlain by ejecta (Fig. 1). This bowl-shaped depression is sometimes referred to as the apparent crater. It is underlain by an allochthonous breccia lens, which is parabolic in cross-section and contained by fractured but mostly autochthonous target rocks (Fig. 1). The crater defined by the parautochthonous target rocks is referred to as the true crater. At larger diameters, collapse features in the rim area become more prominent, and the structure evolves into a so-called complex structure, which consists of a structurally complex rim, a downfaulted annular trough, and a structurally uplifted central area (Fig. 2).

[1] Geological Survey of Canada, 1 Observatory Crescent, Ottawa, Canada K1A 0Y3. Contribution 34795 from the Geological Survey of Canada.

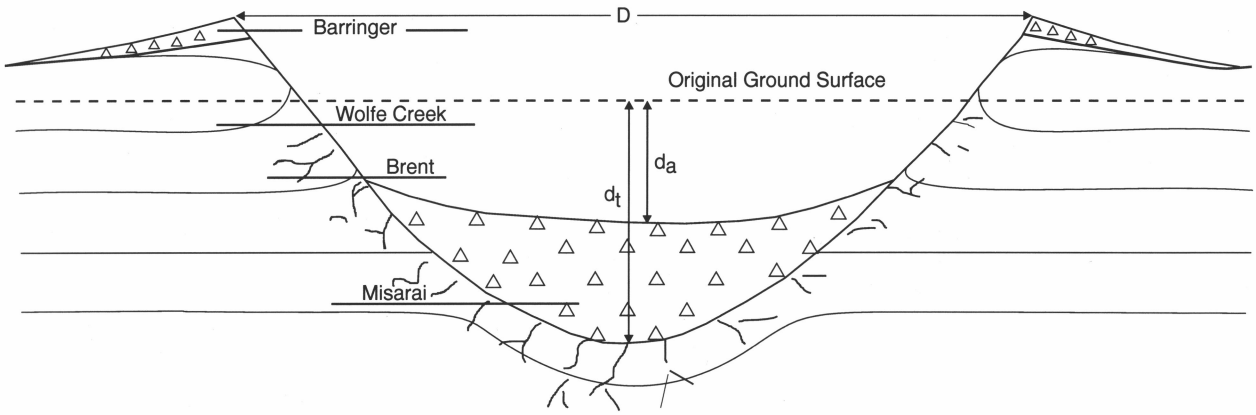

Figure 1. Schematic cross-section of a simple impact structure. Note the overturned flap on the rim overlain by ejecta (small triangles), and the interior allochthonous breccia (large triangles) partly filling the true crater. Present erosional levels of a number of terrestrial simple craters (Table 1) are indicated on the left side of the structure. Definitions of rim diameter (D), apparent depth (d_a), and true depth (d_t) are also indicated.

Table 1. Principal characteristics of terrestrial impact structures mentioned in the text

Structure	*Country*	*Latitude*	*Longitude*	*Diameter (km)*[a]	*Age (Ma)*[a]
Acraman	Australia	32°01'S	135°27'E	85–90	~590
Ames	USA	36°15'N	98°12'W	16	470 ± 30
Avak	USA	71°15'N	156°38'W	12	>95
Barringer	USA	35°02'N	111°01'W	1.2	0.049 ± 0.003
Boltysh	Ukraine	48°45'N	32°10'E	24	88.3
Bosumtwi	Ghana	6°30'N	1°25'W	10.5	0.3 ± 0.02
Brent	Canada	46°05'N	78°29'W	3.8	450 ± 30
Charlevoix	Canada	47°32'N	70°18'W	54	357 ± 15
Chesapeake Bay	USA	37°15'N	76°04'W	85	35.5 ± 0.6
Chicxulub	Mexico	21°20'N	89°30'W	180	64.98 ± 0.05
Connolly	Australia	23°22'S	124°45'E	9	<60
Couture	Canada	60°08'N	75°20'W	8	430 ± 25
Dellen	Sweden	1°55'N	16°39'E	8	89.0 ± 2.7
East Clearwater	Canada	56°05'N	74°07'W	26	290 ± 20
Gardnos	Norway	60°39'N	9°00'E	5	500 ± 10
Gosses Bluff	Australia	23°49'S	132°18'E	24	142.5 ± 0.5
Haughton	Canada	75°22'N	89°41'W	24	23 ± 1
Kara	Russia	69°12'N	65°00'E	65	73 ± 3
Lockne	Sweden	63°00'N	14°48'E	7	455
Misarai	Lithuania	54°01'N	24°34'E	3	570 ± 50
Mistastin	Canada	55°53'N	63°18'W	28	38 ± 4
Mjølnir	Norway	73°48'N	29°40'E	40	143 ± 20
Montagnais	Canada	42°53'N	64°13'W	45	50.5 ± 0.8
Puchezh-Katunki	Russia	57°06'N	43°35'E	80	220 ± 10
Ries	Germany	48°53'N	10°37'E	24	15.1 ± 1
Saint Martin	Canada	51°47'N	98°32'W	40	220 ± 32
Siljan	Sweden	61°02'N	14°52'E	53	368.0 ± 1.1
Slate Islands	Canada	48°40'N	87°00'W	30	<350
Sudbury	Canada	46°36'N	81°11'W	~250	1850 ± 3
Teague	Australia	25°52'S	120°53'E	30	1630 ± 5
Tookoonooka	Australia	27°20'S	142°49'E	~55	128 ± 5
Vredefort	South Africa	27°00'S	27°30'E	~300	2016 ± 10
West Hawk	Canada	49°46'N	95°11'W	2.44	100 ± 50
Wolfe Creek	Australia	19°10'S	127°46'E	0.88	0.3

a. Other diameter and age estimates have been presented for some of these structures — e.g., Sharpton et al. (1993) has estimated the diameter of Chicxulub to be 300 km.

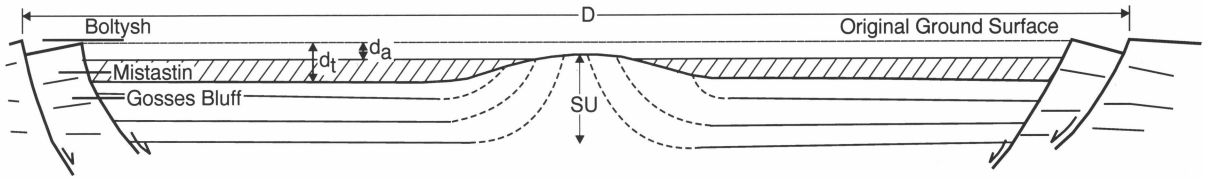

Figure 2. Schematic cross-section of a complex impact structure (not to scale). Note the faulted rim area, downfaulted annular trough, and uplifted centre. Present erosional levels of a number of terrestrial complex impact structures (Table 1) are indicated on the left side of the structure. Rim diameter (D), apparent depth (d_a), true depth (d_t), and amount of stratigraphic uplift (SU) are also indicated. Allochthonous materials (impact-melt rocks and/or breccias) partly filling the structure are indicated by diagonal lines.

Figure 3. Oblique aerial photograph of the 0.88-km-diameter Wolfe Creek Crater (Australia; Table 1), an example of a simple impact structure. Note that this structure, although only ~300 000 years old, has an eroded rim and is partly filled by sediments.

As with simple structures, complex structures are partly filled by allochthonous material, such as breccias and impact-melt rocks, and an apparent and true crater can be defined (Fig. 2). The uplifted central area has initially the topographic form of a central peak, which rises above the floor of the structure (Fig. 2) and has a height that generally does not exceed the depth from the rim to the floor (Pike 1977). With increasing diameter, the central peak is accompanied by a fragmentary ring (a central-peak basin). Larger structures have an interior ring with no peak (a peak-ring basin), and even larger-diameter structures have multiple inner rings (a multi-ring basin; Hartmann & Wood 1971; Wood & Head 1976). These forms and definitions, as well as much of the known morphometry, for the various types of impact structures are based on the planetary, particularly the lunar, record.

These terms are also used to describe terrestrial impact structures (Table 2). There are, however, a number of complicating factors in the terrestrial environment. Few terrestrial impact structures exposed at the surface have near-pristine forms. Near-pristine forms are restricted to the youngest terrestrial impact structures. As smaller impacts occur more frequently than larger ones, they are, therefore, limited to structures with the simple form. The best examples include Barringer (or Meteor) Crater (USA) and Wolfe Creek (Australia; Fig. 3; Table 1). Even they, however, have been modified to some degree by erosion and sedimentary infilling.

Most larger, complex structures are eroded to varying degrees (Fig. 4). There are, however, a number of complex impact structures which were buried by post-impact sediments almost immediately after formation (e.g., Chicxulub, Mexico; Montagnais, Canada; Puchezh-Katunki, Russia; Table 1), and presumably have a near-pristine form. They can, however, only be delineated by drillhole and geophysical data, and therefore the exact details of their morphologies are generally not well known. Only the largest terrestrial impact structures have the potential to be peak-ring basins or multi-ring basins. Unfortunately, the largest structures — Chicxulub; Sudbury, Canada; and Vredefort, South Africa (Table 1) — are either buried, tectonised, or eroded. Their original detailed morphology cannot be defined with confidence, although they are assumed to represent multi-ring or peak-ring basins (e.g., Sharpton et al. 1993; Hildebrand et al. 1995; Spray & Thompson 1995).

There is a tendency to compare terrestrial impact structures with, particularly, lunar impact structures (e.g., Pike 1985), and to assume a greater equivalence in detailed morphology than the observational data would suggest. However, the planetary environments evince important differences. For example, secondary target effects on Earth include the transition from simple to complex forms at diameters of ~2 km and ~4 km, depending on whether the target rocks are sedimentary or crystalline respectively; there are also mixed targets with sediments overlying crystalline basement. Some complex impact structures in mixed or largely sedimentary targets do not appear to develop a topographically high central peak. For example, Ries (Germany) and Haughton (Canada; Fig. 5) are of similar size and age (Table 1) and have no emergent central peak; in contrast, Boltysh (Ukraine; Table 1), which is of a similar size but in a crystalline target, has a central peak that is emergent from the surrounding ~300 m of impact lithologies filling the structure. All these structures have been affected by only minor erosion,

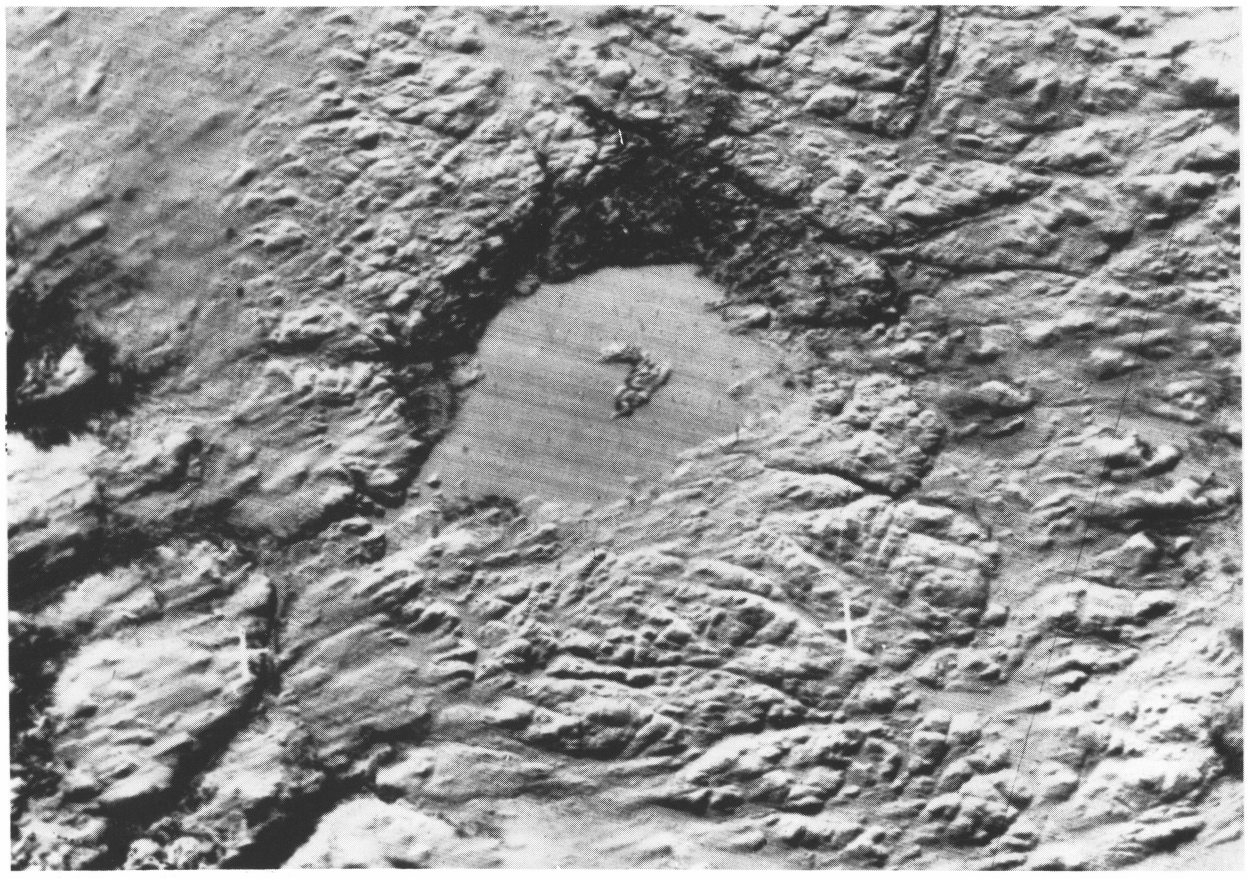

Figure 4. Landsat image of the 28-km-diameter Mistastin (Canada; Table 1) complex impact structure. The central uplift is represented as a 5-km-diameter horseshoe-shaped island; the annular trough is partly occupied by a (frozen) lake; and the rim is barely visible. The relative level of erosion is indicated in Figure 2.

and, at present, there is no clear explanation for this difference in their morphologies.

In addition, planetary gravity has an effect on cratering mechanics and, thus, morphologies. The lower lunar gravity (0.1645 g, where g is the average terrestrial value for gravitional acceleration) results in deeper impact structures on the moon compared with structures of an equivalent size on Earth. This is because gravity is the force acting against both the excavation of material and the formation of topography. In addition, the various forms of impact structures, and their diameter ranges, appear to be an inverse function of planetary gravity (Pike 1985). Thus, they form smaller diameters on Earth than on the moon. There is an additional effect due to gravity. Gravity is a variable in cratering mechanics, but it is not a variable in determining the volume of target material melted in a specific impact event. Thus, an impact into crystalline target rocks generates ~2.5 times more impact melt in a terrestrial than a lunar event resulting in a structure of equivalent size (Cintala & Grieve 1994). This additional melt, which in large part is retained within the impact structure, also has the effect of reducing observed topographic variations.

By far the greatest difference between planetary and terrestrial impact structures, however, is the effect of erosion and sedimentation in the terrestrial environment. Both processes effectively remove impact structures from the terrestrial record by destruction or burial of the craterform. It has been estimated that the signature of a 20-km impact structure can be removed from the record by erosion in <120 Ma if glaciation is one of the erosional agents (Grieve 1984). The effects of erosion are apparent even in low-erosional environments, such as Australia. For example, Wolfe Creek is only ~300 000 years old and occurs within a desert to semi-desert environment (Fig. 3). Nevertheless, it has had its topographic expression in terms of depth reduced by >100 m, or ~70 per cent, according to the present and original topography as constrained by gravity and crater models (Fudali 1979; Grieve et al. 1989). At the present rate of erosion and infilling, Wolfe Creek will cease to exist as a craterform in slightly over 100 000 years. This, however, does not necessarily mean that it would no longer be recognisable as the site of an impact. Impact results in characteristic geological and geophysical effects that are clearly recognisable, even after the original craterform has been removed. As such impact sites are still recognisable but are no longer, by definition, craters, they are referred to as impact structures. In order not to be forced to define when a terrestrial impact crater becomes an impact structure, we refer to all, by the more generic term, as impact structures.

Morphometry

Owing to erosion, few terrestrial impact structures have sufficient topographic information to define morphometric relations. The morphometry of the seven simple structures with the best available data (Grieve et al. 1989) define the relationships:

$$d_a = 0.13D^{1.06}, \text{ and}$$

$$d_t = 0.28D^{1.02},$$

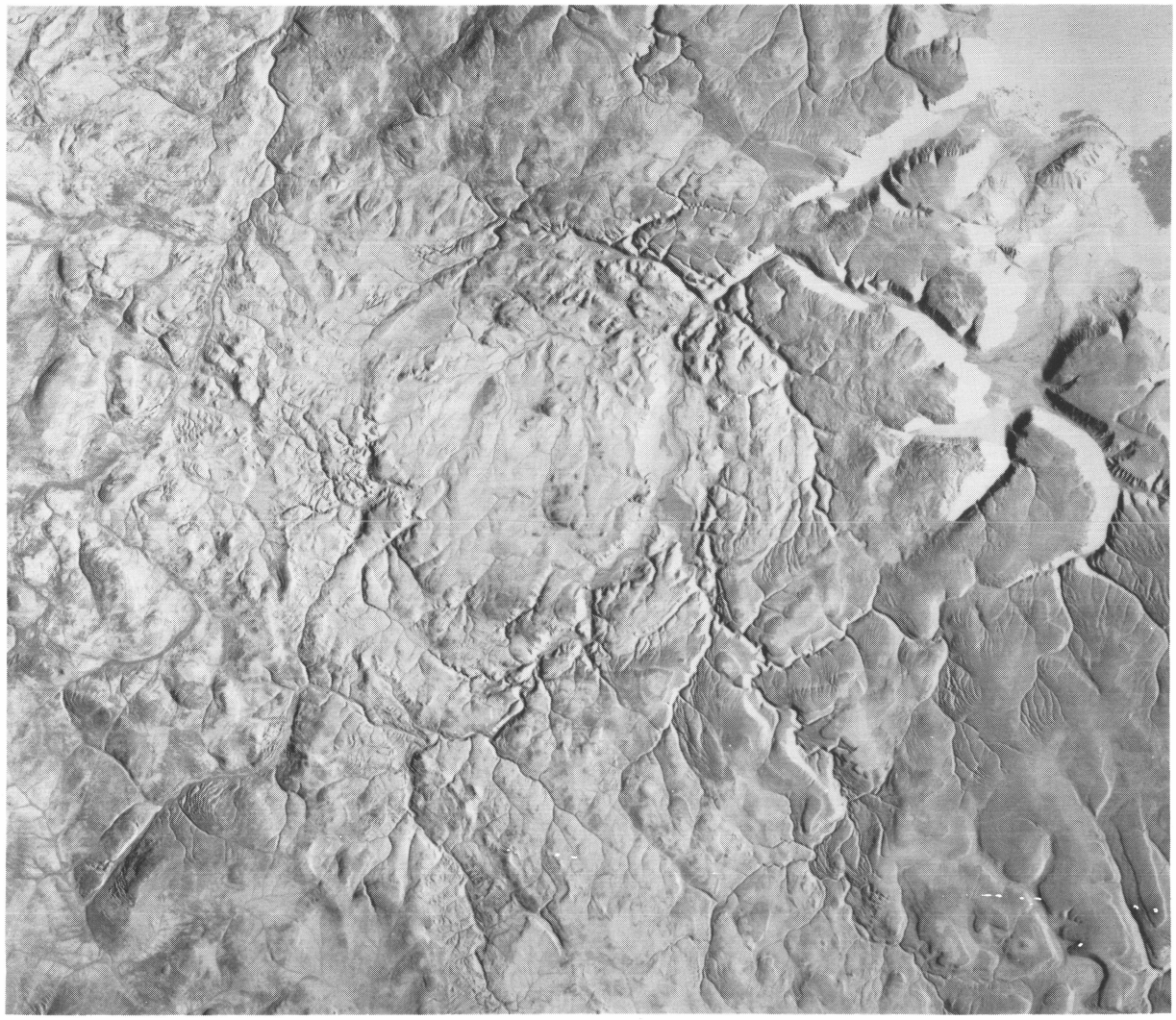

Figure 5. Airborne X-band radar image of the 24-km-diameter complex impact structure at Haughton (Canada; Table 1). Although only slightly eroded, it has no evidence of a topographic central peak (cf. Fig. 4).

where d_a and d_t are the apparent and true depths as measured from the original ground surface to the top and bottom, respectively, of the infilling allochthonous breccia lens; D is the rim diameter as measured at the top of the rim; and units are kilometres (Fig. 1). As noted earlier, the largest terrestrial simple structures in crystalline targets have D ~<4 km. Thus, the amount of erosion required to remove the topographic expression of the largest simple structure on Earth is ~500 m. To remove essentially all geological expression of the structure and the allochthonous breccia lens (Fig. 1), however, requires >1 km of erosion.

There are even fewer good-quality topographic data on the original dimensions of complex structures. Grieve & Pesonen (1992) defined the relationships:

$$d_a = 0.12D^{0.30} \text{ and}$$

$$d_a = 0.15D^{0.43},$$

for sedimentary and crystalline targets respectively (Fig. 2). These relationships are based on data from only five structures and have considerable uncertainty. This uncertainty is due in part to the known examples of larger complex structures being generally older than simple structures, because of the cratering rate, and in part to their smaller d/D ratios (Fig. 2) being more sensitive to topographic changes due to erosion. Nevertheless, the general form of the relationships is similar to that for the moon, where $d_a \propto D^{0.3}$ for lunar complex structures (Pike 1977). On the basis of these relationships, the topography of a 20-km-diameter complex structure would be removed by erosion as little as 300–500 m deep. Like simple structures, such an eroded complex structure would still be recognisable by the geological effects of impact. Indeed, the site of a complex impact structure can be recognised even if it is eroded well below the parautochthonous rocks of the original floor of the structure. The stratigraphic uplift of material in the centre of complex impact structures can be recognised as a geological anomaly (Fig. 2).

The amount of stratigraphic uplift and the diameter of a complex structure maintain a moderately well-defined relationship:

$$SU = 0.06D^{1.1},$$

where SU is the amount of stratigraphic uplift undergone by the deepest lithology now exposed at the surface in the centre (Grieve et al. 1981). This relationship was based on data from 15 complex impact structures. We have revised it, here, according to data from our most recent compilation of terrestrial

Table 2. Morphological and geological signatures of terrestrial impact structures

	Simple	*Complex*
Morphology[a]	Bowl-shaped depression.	Flat floor with faulted rim and central structural uplift, which may be manifested as a topographic peak and/or interior ring(s).
Morphometry[a]	d_t ~$2d_a$ and 1/3 D. D ~<2 and 4 km in sedimentary and crystalline targets respectively.	d:D variable, but less than simple craters and decreasing with D. SU ~1/10 D.
Geology	Partly filled by allochthonous breccia lens with melt rocks. Fractured parautochthonous target rocks, possibly with various breccia and melt dykes.	Partly filled by relatively thin (with respect to D) impact-melt rocks and/or allochthonous breccia. Uplifted deeper lithologies in centre. Downfaulted lithologies in annular trough. Fractured parautochthonous target rocks with various breccia and melt dykes extending out to rim.
Shock metamorphism	In breccia lens; most highly shocked materials are concentrated at top and bottom. In parautochthonous target rocks, shock effects are limited to floor of true crater, and attenuate radially and with depth.	In allochthonous lithologies. In parautochthonous target rocks, shock effects are limited to central uplift (<0.5D), and attenuate radially and with depth.

a. For largely uneroded structures.

impact structures and their characteristics; the relationship is now based on data from 24 structures, and is redefined as:

$$SU = 0.086D^{1.03} \text{ (Fig.6).}$$

Therefore, after the removal of the topography associated with a 20-km-diameter complex structure, the geological expression of the structural uplift requires an additional ~2 km of erosion before it too is removed from the terrestrial record.

Differential erosion has removed all topographic expression of the craterform at a number of complex impact structures, and replaced it with a residual central positive structure. For example, geological and geophysical data indicate that the Gosses Bluff structure is 24 km in diameter (Table 1; Milton et al. this issue; Tingate et al. this issue). The present surface topographic expression of the structure, however, is restricted to a central 4.5-km-diameter annular ridge rising 200 m above the surrounding plain (Fig. 7). This annular ridge represents the remnant core of a central uplift containing erosionally resistant Ordovician–Devonian sandstone. Thus, the present form of Gosses Bluff owes as much to erosion and lithology, as to the original complex crater morphology.

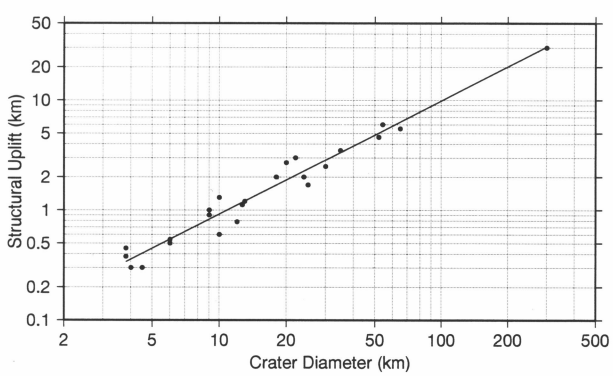

Figure 6. Structural uplift (SU) versus rim diameter (D) for 24 terrestrial complex impact structures in log–log space. Least-squares regression of the data gives the relation SU = 0.086 $D^{1.03}$.

The observation that eroded terrestrial complex impact craters can appear ultimately as neutral or even positive topographic features with uplifted lithologies has contributed historically to the reluctance of some workers to accept the impact origin of certain structures (e.g., Bucher 1963). There has been a recent increase in interest in the contrary hypothesis of a cryptoexplosion origin for certain complex impact craters. This is a direct consequence of the promotion of the argument that the causal agent of the mass extinction and the evidence at the KT boundary are not related to impact (e.g., Loper & McCartney 1988; Carter et al. 1990; Officer 1992). Previously advanced arguments, however, for an impact origin have been elegantly summarised recently by French (1990). These arguments are rooted largely in the geological characteristics of impact structures.

Geology of impact structures

Even though an anomalous circular topographic, structural, or geological feature may indicate the presence of an impact structure, there are other endogenic geological processes that can produce similar features in the terrestrial environment. An obvious craterform is an excellent indicator of a possible impact origin, particularly if it has the appropriate morphometry, but, as noted earlier, such features are rare and short-lived in the terrestrial environment. The burden of proof for an impact origin generally lies with the documentation of the occurrence of shock-metamorphic effects.

Few structures preserve physical evidence of the impacting body. They are limited to small, young, simple structures, where the impacting body (or fragments of it) has been slowed by atmospheric retardation, and impacts with less than its cosmic velocity. These are restricted generally to the impact of iron or stony-iron meteorites. Stony meteorites are weaker than their iron-bearing counterparts, and small ones are generally crushed in the atmosphere as a result of atmospheric interaction and the formation of a stress gradient from their leading to trailing edges (Melosh 1981). Larger impacting bodies (>100–150 m in diameter) survive atmospheric passage with undiminished velocity. Consequently, the peak shock pressures upon impact

Figure 7. Oblique aerial photograph of Gosses Bluff (Australia; Table 1). This 24-km-diameter complex impact structure is eroded below the original floor (Fig. 2), and is now expressed as a 4.5-km-diameter topographically positive annulus of hills due to differential erosion.

are sufficient to result in the vaporisation of the impacting body, destroying it as a physical entity.

Shock metamorphism is the progressive breakdown in the structural order of rocks and, more importantly, their constituent minerals, and is caused by the passage through them of a high-pressure shock wave. On impact, the bulk of the impacting body's kinetic energy is transferred to the target by means of a shock wave. This shock wave imparts kinetic energy to the target materials, which leads to the formation of a crater, and increases the internal energy of the target materials, which leads to the formation of shock-metamorphic effects. The details of the physics of impact and shock-wave behaviour, including cratering mechanics, are presented by Melosh (1989, and references therein), and are not repeated here.

Shock-metamorphic effects observed at terrestrial impact structures, and in shock-recovery experiments, are the net result of transient compression by the shock wave and then release to ambient pressure. Considerable pressure–volume work is done during compression, and pressure release is along an adiabat. Not all the pressure–volume is recovered on release, and the excess is manifested as waste-heat. The amount of trapped waste-heat increases with increasing shock pressure, and ultimately leads to the melting and vaporisation of a portion of the target rocks and, as noted previously, the impacting body. The exact physical conditions on impact are a function of the specific impact parameters. The density of the impacting body and the target, and the impact velocity, determine the peak pressure, which can be considerable. For example, the impact of a stony chrondritic body into granite at 25 km s^{-1} results in a peak pressure at the point of impact of ~900 GPa (9 million bars). The intensity of the shock wave attenuates with distance into the target, and the size of the impacting body determines the absolute radial distance in the target at which a specific shock pressure is achieved and, thus, at which shock-metamorphic effects occur.

Shock-metamorphic effects are well-described in papers in French & Short (1968) and Roddy et al. (1977), as well as by Stöffler (1971, 1972, 1974). They are discussed here only in general terms. Minimum shock pressures required for the production of diagnostic shock-metamorphic effects are 5–10 GPa for most silicate minerals. Shock metamorphism occurs at extremely high strain rates (~10^6–10^9 s^{-1}), and shock-pressure duration is measured in seconds, or less, in even the largest impact events (Melosh 1989). Thus, unlike endogenic terrestrial metamorphism, disequilibrium and metastability are common phenomena in shock metamorphism.

The only known diagnostic shock effect that is megascopic in scale is the occurrence of shatter cones (Dietz 1968). These conical striated fracture surfaces are best developed in fine-grained, structurally isotropic lithologies, such as carbonates and quartzites (Fig. 9). They do occur in coarse-grained crystalline rocks but are less common and poorly developed. Shatter cones are initiated most frequently in rocks that experienced moderately low shock pressures, 2–6 GPa, but have been observed in rocks that experienced ~25 GPa (Milton 1977). All other diagnostic, subsolidus, shock-metamorphic effects are microscopic in scale.

The most common documented shock-metamorphic effect is the occurrence of so-called planar microstructures in tectosilicates, particularly quartz (Hörz 1968). The utility of planar microstructures in quartz reflects the ubiquitous nature of the mineral and its stability, and the stability of the microstructures themselves, in the terrestrial environment, and the relative ease with which they can be documented. Planar elements in quartz are divided into planar fractures (PFs) and planar deformation features (PDFs). PDFs (Figs 8 and 9) are most common in crystalline targets, and, when fresh, most are filled with glass (Engelhardt & Bertsch 1969). These glass lamellae are moderately easily annealed, and are commonly manifested as linear chains of inclusions and bubbles, called decorated planar features, which are observed at all but the youngest impact structures. PDFs in quartz have specific orientations, which are a function of recorded shock pressure, and have been calibrated in large part by shock-recovery experiments. Major recent reviews of the nature of the shock metamorphism of quartz, with an emphasis on the nature and origin of planar microstructures in experimental and natural impacts, can be found in Stöffler & Langenhorst (1994) and Grieve et al. (1996).

The development of PDFs in quartz, which occurs over the pressure range of 5–10 to ~35 GPa, is accompanied by progressive changes in other optical and physical properties (Stöffler &

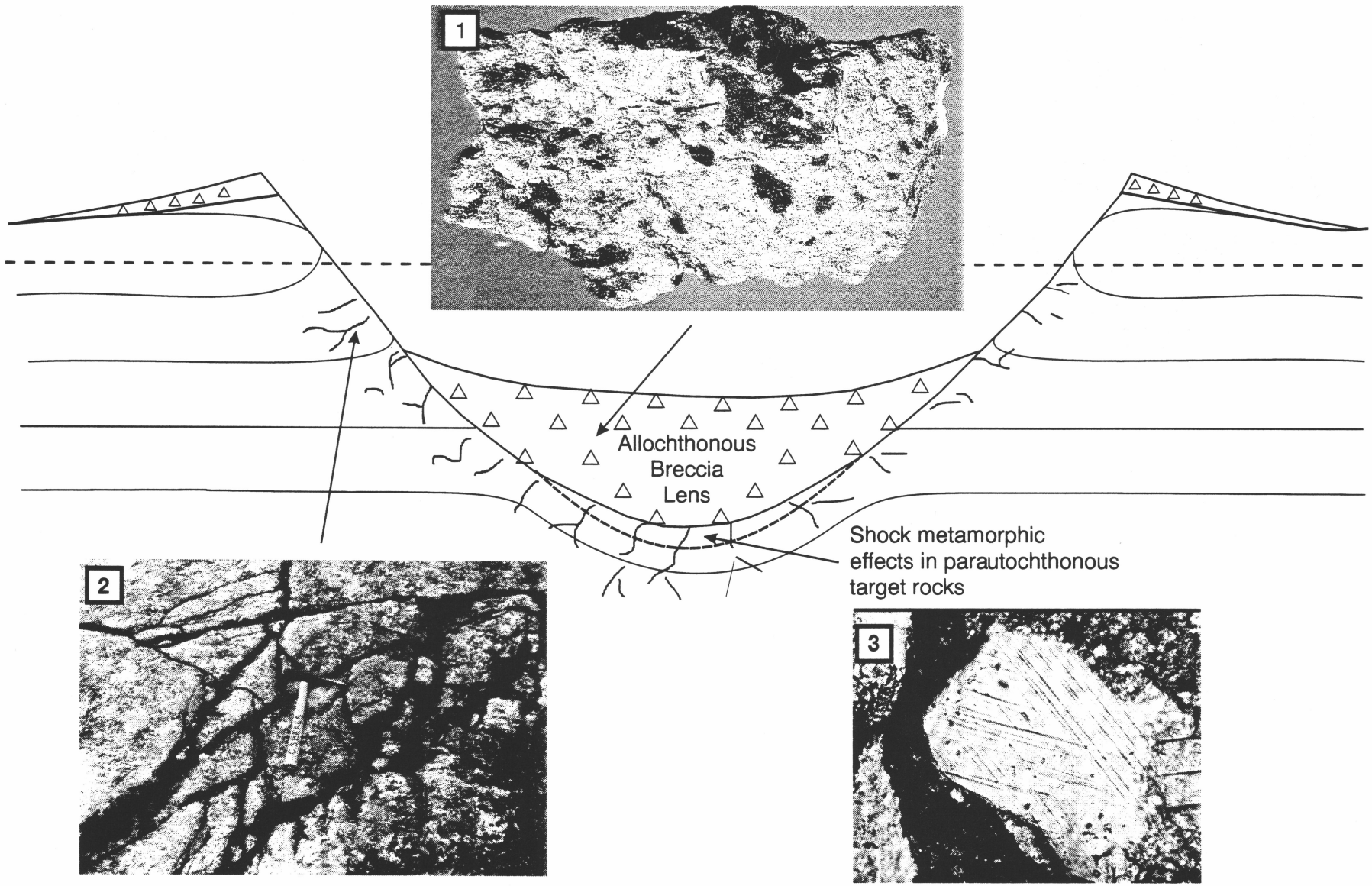

Figure 8. Schematic cross-section of a terrestrial simple impact structure, and the locations and nature of various shock-metamorphic effects: (1) allochthonous breccia with clasts (dark) of impact-melted target rock; (2) fractured parautochthonous target rock of the wall of the true crater; (3) planar deformation features in parautochthonous target rocks of the floor of the true crater.

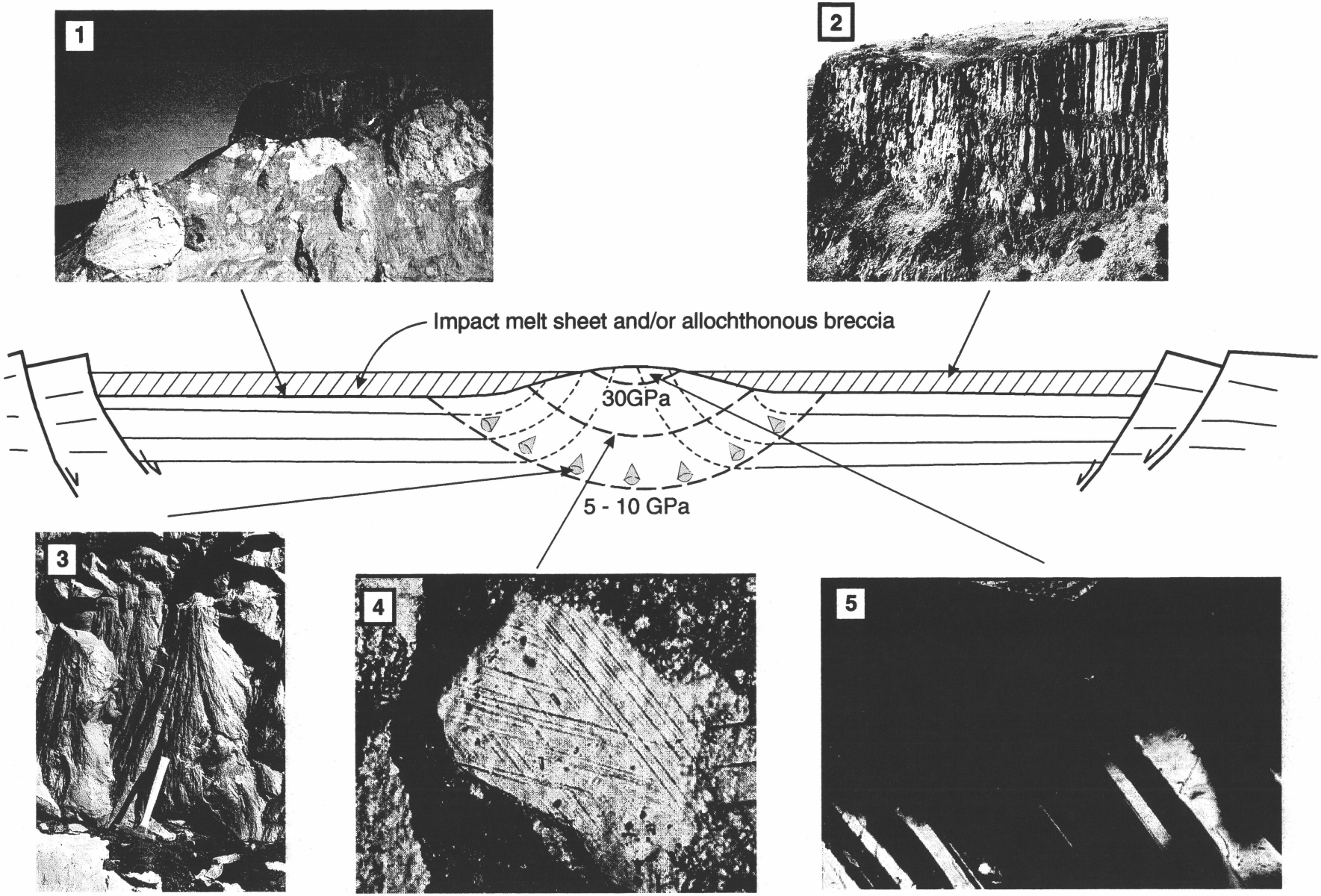

Figure 9. Schematic cross-section of a terrestrial complex impact structure, and the locations and nature of various shock-metamorphic effects: (1 and 2) allochthonous coherent impact-melt sheet overlying allochthonous breccia; (3) shatter cones; (4) planar deformation features in quartz; (5) development of diaplectic glass in feldspar. Also indicated are the general positions of shock isobars in parautochthonous target rocks of the central uplift. Note the spatial confinement of these shock effects to the centre of the structure, and their attenuation radially and with depth.

Langenhorst 1994). For example, asterism and line broadening — apparent from X-rays — reveal a progressive breakdown in structural order (e.g., Chao 1968; Hörz & Quaide 1973; Hanss et al. 1978).

Porous sedimentary rocks evince some differences in the response to shock compared with crystalline or compact sedimentary rocks. For example, quartz in sandstone exhibits more PFs and fewer PDFs, and certain PDF orientations, such as ω {10$\bar{1}$3}, tend to be suppressed relative to PDFs in quartz in shocked crystalline rocks (Fig. 10; Robertson 1980; Grieve & Therriault 1995). In addition, during shock compression, considerable pressure–volume work is done in collapsing pore space. As a result, more waste-heat is trapped in porous sedimentary rocks than in crystalline rocks shocked to equivalent pressure. This leads to enhanced intra- and inter-mineral melting at moderately low shock pressures. Details of some of these effects, as observed in the Coconino Sandstone at the Barringer structure, are presented by Kieffer (1971) and Kieffer et al. (1976).

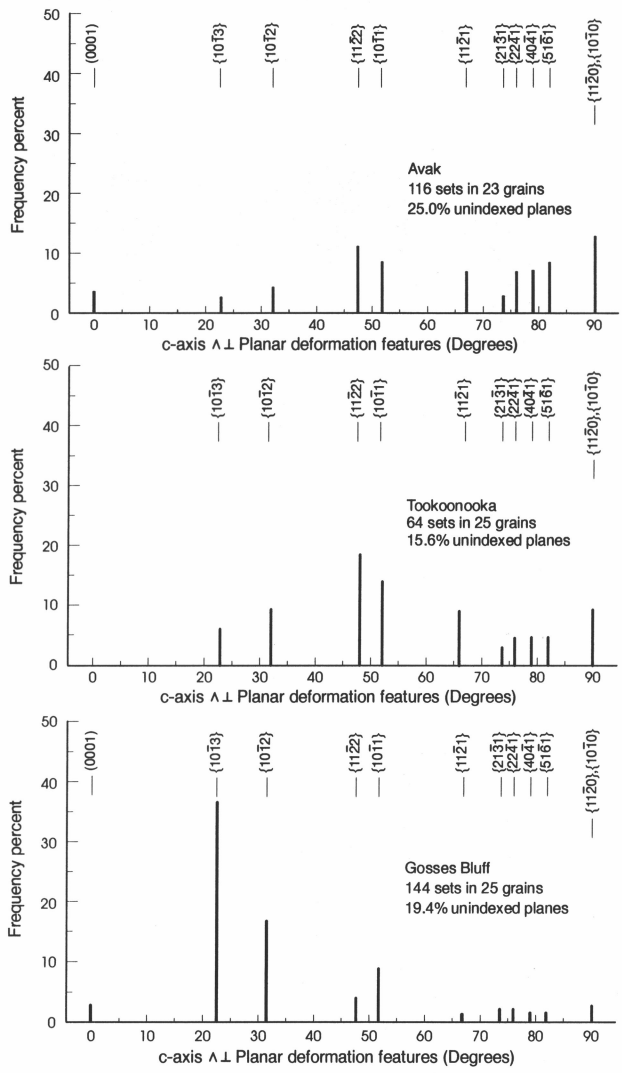

Figure 10. Frequency per cent of indexed orientations of planar deformation features in quartz from Avak (USA; Table 1), Tookoonooka (Australia; Table 1), and Gosses Bluff. Note the relative shortage of ω {10$\bar{1}$3} orientations at Avak and Tookoonooka compared with Gosses Bluff. This is believed to be a textural effect peculiar to porous sedimentary rocks.

The reason why certain orientations of PDFs in quartz are suppressed in porous sedimentary rocks is not known and is the subject of current study. Robertson (1980) suggested that, in the pressure range in which — for example — ω features are formed in crystalline rocks, PDFs do not form in porous sedimentary rocks, as the pressure–volume work due to compression is being adsorbed in closing pores. Clearly, these second-order differences in the behaviour of rocks subjected to shock are related to textural differences. For example, the relative abundances of certain PDF orientations in different sandstone units at Gosses Bluff are texture-dependent: units with an equigranular close-packed texture have relative orientation abundances similar to crystalline rocks (Fig. 10); others with more isolated quartz grains in a fine-grained matrix are similar, with respect to PDF orientations, to other more porous sandstones at other impact structures (Grieve et al. 1996).

Shock pressures of ~30 and ~35 GPa are sufficient to render feldspar and quartz, respectively, to glasses (Fig. 9). These are solid-state glasses with physical properties distinct from fusion glasses, and are generally referred to as a diaplectic glass (Stöffler & Horneman 1972). In addition, shock can result in the formation of metastable polymorphs, such as stishovite and coesite from quartz (Chao 1968) and diamond and lonsdaleite from graphite (Masaitis et al. 1972). Coesite and diamond are also products of endogenic terrestrial geological processes, including high-grade metamorphism (e.g., Dobrzhinetskaya et al. 1995), but the paragenesis and, more importantly, the geological setting are completely different.

By ~50 GPa individual minerals begin to decompose thermally or melt (Stöffler 1972, 1984), leading to the production of mixed mineral melts. Above ~60 GPa, the waste-heat is sufficient to result in whole-rock melting. Such melts occur as glass bombs in crater ejecta (Engelhardt 1990), as glassy to crystalline fragments and lenses in breccias (Fig. 8), and as coherent sheets (Fig. 9; Grieve et al. 1977). When crystallised, impact-melt sheets have igneous textures, but tend to be heavily charged with clastic debris towards their lower and upper contacts. They may, therefore, have a textural resemblance to endogenic igneous rocks. Impact-melt rocks, however, commonly have an unusual chemistry compared with endogenic volcanic rocks, as their composition depends on the melting of a mix of target rocks, as opposed to partial melting and/or fractional crystallisation relationships that apply to igneous rocks. Isotopic analyses also indicate that such parameters as $^{87}Sr/^{86}Sr$ and $^{143}Nd/^{144}Nd$ ratios reflect the pre-existing target rocks, while isochron dating methods indicate much younger crystallisation ages, which are related to the impact event (Jahn et al. 1978; Faggart et al. 1985).

Enrichments above target rock levels in siderophile elements and Cr have been identified in some impact-melt rocks (Palme 1982). These are due to an admixture of up to a few per cent of meteoritic material from the impacting body. In some such rocks, the relative abundances of the various siderophiles have constrained the composition of the impacting body to the level of meteorite class — for example, East Clearwater (Canada; Table 1), which was formed by a Cl chondrite (Palme et al. 1979). In other such rocks, no siderophile anomaly has been identified. This may be due to the inhomogeneous distribution of meteoritic material within the impact-melt rocks and sampling variations (Palme et al. 1981), or to differentiated non-siderophile-enriched impacting bodies, such as basaltic achondrites (Wolf et al. 1980). Most recently, high-precision

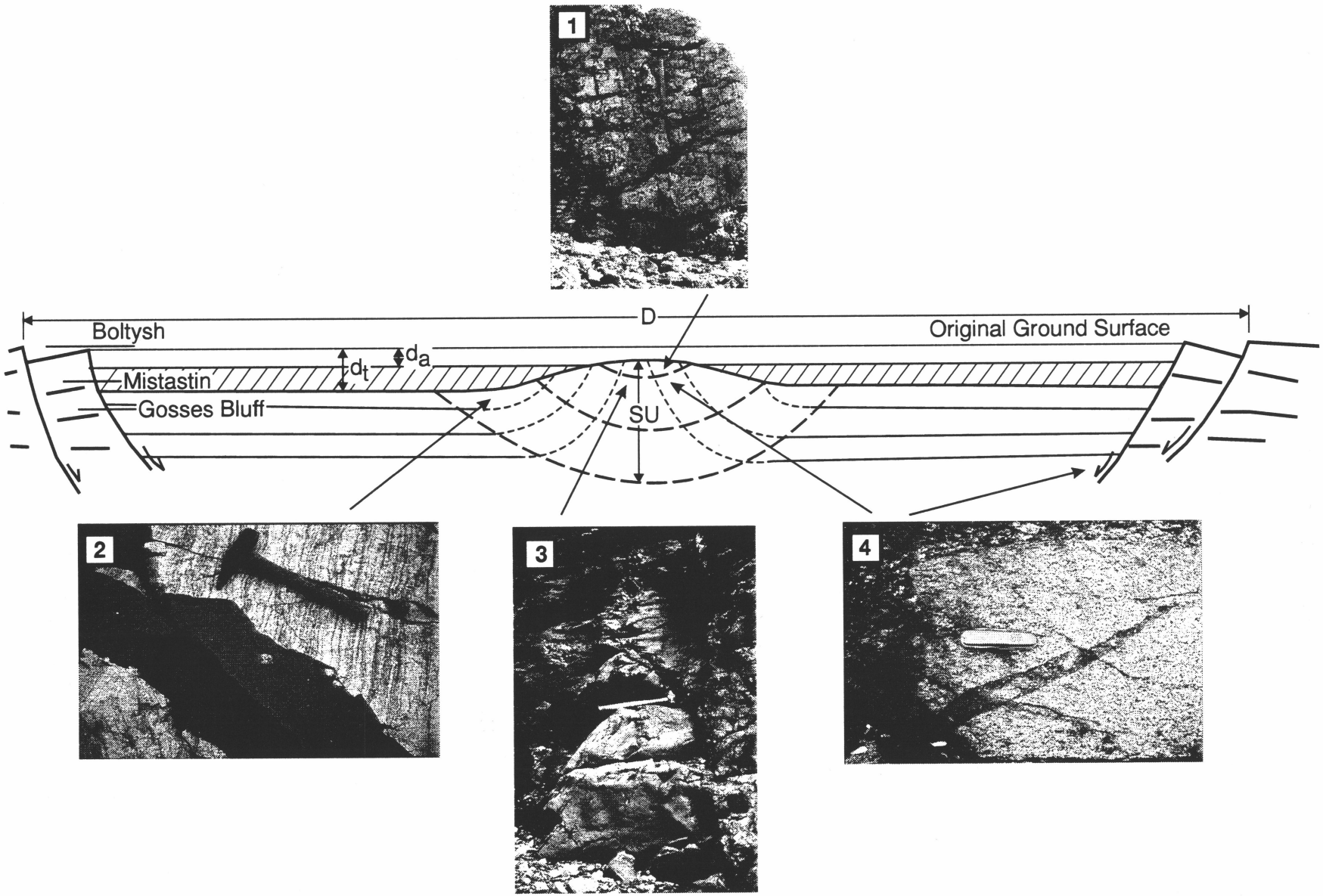

Figure 11. Schematic cross-section of a terrestrial complex impact structure, and the locations and nature of various impact-related lithologies in the parautochthonous rocks of the floor and central uplift: (1) vertically dipping uplifted beds in the central uplift; (2) impact-melt dyke in the floor; (3) clastic breccia dyke in the central uplift; (4) pseudotachylite in the central uplift. Pseudotachylite is also found associated with rim faults.

osmium-isotopic analyses have been used to detect a meteoritic signature at terrestrial impact structures (Koeberl et al. 1994). The sensitivity of this isotopic technique might help detect additional, faint meteoritic signals in impact lithologies. Osmium-isotopic ratios are, however, ineffective for discriminating between types of meteoritic bodies.

The proportion of recognisable impact-melt rocks at craters in sedimentary and some mixed targets is at least two orders of magnitude less than at similar-size terrestrial craters in crystalline targets (Kieffer & Simonds 1980). A polymict allochthonous breccia deposit in sedimentary targets occupies the equivalent stratigraphic position to an impact-melt sheet in crystalline targets (Fig. 9). These breccia deposits can contain highly shocked melted clasts and glass corresponding in composition to target rock sedimentary lithologies (Redeker & Stöffler 1988). These deposits are generally referred to as suevitic breccias, particularly by workers from the former USSR (Masaitis et al. 1980). Like the suevite deposits of Ries, which is in a mixed target and where the compositions of the melt glasses correspond to the underlying crystalline target rocks (Pohl et al. 1977; Stöffler et al. 1977), they contain clasts showing all levels of shock.

The lack of extensive coherent sheet-like impact-melt deposits at structures in sedimentary targets is perhaps unexpected, as theoretical considerations indicate that sedimentary lithologies melt under shock compression at equivalent, or even lower, shock pressures than crystalline lithologies. This absence, however, is not a function of the melting behaviour of the various target rock lithologies, but is believed to be due to the extensive expansion of volatiles from sedimentary rocks on their release from shock compression (Kieffer & Simonds 1980). For example, shock experiments indicate that ~50 per cent of the carbon dioxide in calcite is volatilised by shock pressures as low as 30 GPa (Lange & Ahrens 1986). Thus, the impact melt in sedimentary impacts is highly dispersed by gas expansion, which results in the production of mainly impact-melt-bearing suevitic breccia deposits instead of a coherent impact-melt sheet. In addition, the presence of volatiles results in enhanced alteration of the impact-melt glasses to carbonates and hydrated phases.

In addition to extensive deposits of polymict allochthonous breccia, other types of breccia are found at terrestrial impact craters. They include various types of dykes of allochthonous monomict and polymict breccias (Fig. 11) related to various stages of crater formation (Lambert 1981; Stöffler et al. 1988). Also, a large volume of mostly autochthonous monomict breccia and fractured target rocks make up the floor of impact structures. Pseudotachylite is also present at craters in crystalline targets (Fig. 11), the most spectacular occurrences being at Vredefort and Sudbury, where these frictional melt breccias occur over areas of ~5000 km^2 (Dressler 1984; Reimold & Colliston 1994). Pseudotachylite and various breccia deposits are characteristic of the geology of terrestrial impact structures. They are, however, not in themselves diagnostic indicators of impact, as they can be formed by other high-strain-rate endogenic geological processes. It is the occurrence of shocked clasts within these lithologies that designate them as being of impact origin.

Distribution of shock metamorphism

As cratering mechanics and shock metamorphism are largely governed by physics, the spatial distribution of shock-metamorphic effects at terrestrial impact structures is essentially invariant. There have been, however, few systematic and detailed studies of the variation in the recorded level of shock at impact structures. Nevertheless, the studies that have been conducted provide a moderately consistent picture of the spatial distribution of shock effects at terrestrial impact structures. In allochthonous lithologies, such as breccias and melt rocks, there can be a wide range of shock effects, ranging from none to melting in close spatial proximity. Apart from ejecta, which are rarely preserved in the terrestrial environment, such allochthonous lithologies are confined to within the rim and floor of both simple and complex impact structures (Figs. 8 and 9).

Short (1970) used PDFs in quartz as a parameter to create a 'shock index' for the allochthonous breccia lens at the simple West Hawk structure (Canada; Table 1). From the shock index, he noted a variation in the level of shock metamorphism; maximum shock levels occurred towards the top and base of the breccia lens. The shock-metamorphic effects in the breccia lens at Brent (Canada; Table 1) are similarly disposed (Dence et al. 1977; Grieve 1978). Most of the material in the breccia lenses at simple impact structures, however, does not display obvious shock-metamorphic features, and the range of shock levels is consistent with the allochthonous nature of the breccias. The concentrations of more highly shocked materials towards the base and upper zones in the centre are due to movements associated with the mechanics of cratering (e.g., Dence et al. 1977; Grieve et al. 1977; Melosh 1989).

To our knowledge, there has been only one example of a systematic study of variations in recorded shock in the parautochthonous rocks beneath a simple impact crater, and this is at Brent (Dence 1968; Dence et al. 1977; Robertson & Grieve 1977). Shock effects occur in the parautochthonous rocks of the floor of the impact structure only in the centre (Fig. 8). For ~15 m beneath an impact-melt lens at the base of the allochthonous breccia lens, all indications of shock metamorphism have been recrystallised. Below this depth, however, PDFs in quartz are apparent but progressively decrease in abundance with depth. Estimates of the shock pressures recorded by the PDFs range from 23.0 to 5.7 GPa over the 85 m where PDFs are apparent (Robertson & Grieve 1977).

At complex impact structures, such as Charlevoix and the Slate Islands (Canada; Table 1), variations in the orientations of PDFs in quartz indicate that recorded shock levels in the parautochthonous rocks of the crater floor attenuate from ~25 GPa at the centre to <5 GPa at radial distances of <0.5 the rim diameter (Fig. 9; Robertson & Grieve 1977). These estimates represent lower bounds, as both structures have been eroded below the original floor, but they do emphasise the observation that shock-metamorphic effects in parautochthonous target rocks of complex structures are, like those at simple structures, spatially limited to the central area, well within the original rim (Fig. 8 and 9). These types of relationships permit the relative spatial limitation of recorded shock to be used to estimate original morphological parameters at severely eroded structures, where there is little or no indication of the original rim. This has been done most recently at very large eroded complex structures, such as Sudbury (Grieve et al. 1991; Deutsch & Grieve 1994; Stöffler et al. 1994) and Vredefort (Therriault et al. 1993, 1995).

Systematic studies of variations in recorded shock with depth at complex structures are limited. There are generally few drill-cores of sufficient depth. Studies at the Ries structure indicate that the recorded shock pressure attenuates over the sampled ~600 m in the crystalline basement floor of the structure (Engel-

hardt & Graup 1977). They also indicate structural complexities with depth and that, as a whole, the section consists of parautochthonous materials which are faulted and displaced. Similarly, the recorded shock pressure, as determined from PDF orientation in quartz, decreases with depth in the parautochthonous rocks of the uplifted floor of the Kara structure (Sazonova 1981; Sazonova et al. 1981; Gurov & Gurova 1991). At the Puchezh-Katunki structure (Russia; Table 1), where samples from 5 km of core drilled in the centre are available (Pevzner et al. 1992), the estimated recorded shock-pressure levels decrease from ~40 GPa at the top of the central uplift to ~10 GPa at 5-km depth, and are, again, largely based on variations in PDF orientations in quartz (Ivanov 1994).

Systematic studies of the distribution of shocked quartz within ejecta are restricted to the Ries structure. In general, a decrease of the recorded shock level from top to bottom of the ejecta has been observed (Pohl et al. 1977; Schneider 1971). Suevite breccia is present on top. It contains abundant impact-melt bombs, and ranges down in recorded shock levels to quartz with coesite and stishovite to quartz with PDFs and PFs of the lowest shock stage or no evidence of shock. This assemblage changes discontinuously at the base of the suevite, where a second polymict breccia unit (called Bunte breccia at Ries) forms the main mass of the ejecta. Schneider (1971) found that the maximum shock level below the suevite is represented by diaplectic quartz glass, and that the abundance of quartz with PFs and PDFs continuously decreases with increasing depth in the Bunte breccia. A more recent study, however, failed to record any systematic distribution in the level of shock metamorphism in the Bunte breccia (Banholzer & Hörz 1979).

There have been no systematic studies of the spatial distribution of recorded shock at impact structures in (porous) sedimentary targets. The most comprehensive work is at Barringer (Kieffer 1971; Kieffer et al. 1976), and it concentrated on establishing a shock classification scheme for various shock-metamorphic effects in the Coconino Sandstone. All samples, however, were allochthonous in nature, and the highest levels of average recorded shock were apparent in the uppermost materials, which are considered to be samples of fall-back breccia.

Disregarding tektite and microtektite occurrences, we know of only two examples in which highly dispersed and well-removed ejecta are linked to a known impact site:

- ejecta from the Acraman structure (Australia; Table 1), which occur up to ~500 km from the impact site (Gostin et al. 1986; Wallace et al. this issue); and
- ejecta from the Chicxulub structure, which occur worldwide at the KT boundary (Bohor et al. 1984, 1987; Hildebrand et al. 1991).

A layer containing shocked quartz and shatter-cone fragments in dacite clasts in the shales of the Adelaide Geosyncline (South Australia) was the initial evidence for ejecta from the Acraman structure. Later work indicated an associated siderophile anomaly (Gostin et al. 1989; Wallace et al. 1990). There is very little documentation on the shock-metamorphic effects, except that the ejecta are PDFs (Gostin et al. 1986).

The initial indications of an impact origin for deposits at the KT boundary were geochemical (Alvarez et al. 1980; Ganapathy 1980). They were followed by the discovery of physical evidence of impact in the form of quartz with PDFs in KT boundary samples from the western interior of North America (Bohor et al. 1984). In addition to PDFs, some quartz grains in the KT boundary layer display reduced refractive indices and X-ray asterism (Bohor 1990), and coesite and stishovite have been identified (McHone et al. 1989; Boslough et al. 1995). Since the initial discoveries, quartz with PDFs, and other shocked minerals, have been recognised worldwide in KT boundary deposits (Bohor et al. 1987).

No systematic study has been undertaken to determine if there is any variation with location in the orientation of PDFs, and thus in the recorded shock pressure, in quartz from KT boundary layers worldwide. The maximum dimensions of the shocked quartz grains, however, tend to be larger and more of them contain PDFs at North American sites than elsewhere (Bohor et al. 1987), suggesting an impact site close to the Americas. This was confirmed by the discovery of the Chicxulub impact structure on the Yucatan Peninsula (Hildebrand et al. 1991).

There have been claims of shock-metamorphic effects in minerals from other biostratigraphic boundaries — e.g., Triassic–Jurassic (Badjukov et al. 1987; Bice et al. 1992). The observation basis for these claims, however, is not as strong as for the KT boundary event. Indeed, the observations are somewhat confusing, because the 'shocked' quartz at the Triassic–Jurassic boundary, for example, occurs in three separate beds (Bice et al. 1992). Recently, however, shocked quartz with PDFs, confirmed by both optical and TEM observations, has been recognised near the Eocene–Oligocene boundary at Massignano (Italy; Langenhorst & Clymer 1995).

There is other evidence of impact in the stratigraphic column. Most often, this is in the form of regional to local occurrences of tektite and microtektite bodies. Some of them are related to known impact structures — e.g., the moldavite tektites with Ries, and the Ivory Coast microtektites with Bosumtwi (Ghana; Table 1). The sources of other strewn fields is unknown, although there are a number of suggestions in the literature (e.g., Wasson 1991; Poag et al. 1994). Some of these strewn fields cover a considerable area of the Earth's surface. For example, the Australasian strewn field covers an area in excess of 50×10^6 km^2 (Koeberl 1994). A recent summary of evidence for impact in the stratigraphic column can be found in Grieve (1996a).

Geophysics of impact structures

Geophysical anomalies over terrestrial impact structures (Table 3) vary in their character and, in isolation, do not provide definitive evidence for an impact origin. About 30 per cent of known terrestrial impact structures are buried by post-impact sediments, and geophysical methods have provided the means for their initial discovery and subsequent exploration. Interpretation of a single geophysical data set over a suspected structure can be ambiguous but, when combined with complementary geophysical methods and the existing database over other known impact structures, a more definite assessment can be made. Since potential-field data are available over large areas, with almost continuous coverage (compared with seismic reflection lines), gravity and magnetic observations are the primary geophysical indicators used for evaluating the occurrence of possible terrestrial impact structures. Seismic data, although providing much better spatial resolution of subsurface structure, is used less, because it is generally unavailable. Electrical methods have been used even less, although they hold promise (e.g.,

Henkel 1992). Several recent discoveries of terrestrial impact structures were identified initially as geophysical anomalies — e.g., Chicxulub (Hildebrand et al. 1991), Mjølnir (Barents Sea; Table 1; Gudlaugsson 1993), and Chesapeake Bay (USA; Table 1; Poag et al. 1994). Their impact origin was confirmed, however, through geological evidence — i.e., the documented occurrence of shock-metamorphic effects.

Gravity signature

The most notable geophysical signature associated with terrestrial impact structures is a negative gravity anomaly (Fig. 12). When the regional fields are removed, these gravity lows are generally circular and extend to, or slightly beyond, the rim of the structure. They are due to the lithological and physical changes associated with the impact process. In uneroded structures, low-density sedimentary infill of the topographic depression of the crater contributes to the gravity low. In complex structures, low-density impact-melt sheets also can contribute to the negative gravity effect. Such lithological effects, however, are minor compared with density contrasts induced by fracturing and brecciation of the target rocks. Porosity levels within the allochthonous breccia deposits increase owing to the fragmentation and redistribution of target lithologies during crater formation. Shock-induced fracturing of parautochthonous target rocks beneath the crater floor also leads to increased porosity and, hence, reduced densities, compared with the surrounding undisturbed formations.

The amplitude of the maximum negative gravity anomaly associated with impact structures increases with the crater diameter (Fig. 13; Dabizha & Fedynsky 1975). The value of this negative anomaly is primarily determined by the density contrast and depth of the brecciated and fractured zones. The final character of the gravity anomaly at largely uneroded structures is determined by D and, to a lesser extent, the pre-impact density distribution of the target rocks. Post-impact processes, such as erosion, may cause further changes in anomaly shape and size. According to the data from 58 terrestrial impact structures, Pilkington & Grieve (1992) showed that erosional level and nature of target lithology (whether mainly sedimentary or crystalline) have only a secondary effect on gravity anomaly size. Erosional effects are most prominent when the structure has been eroded

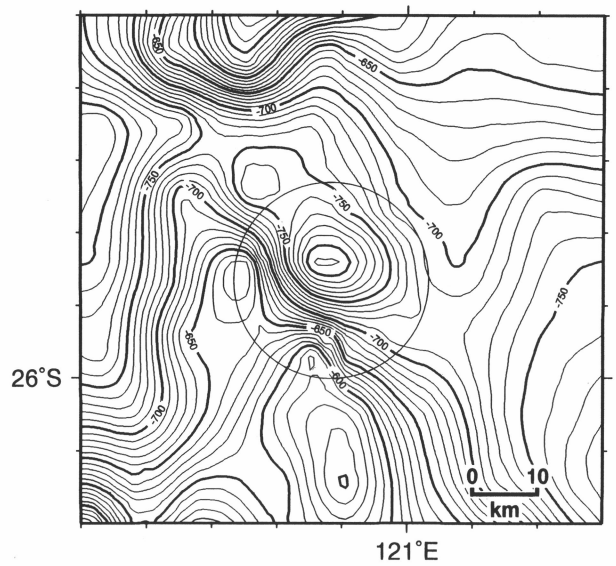

Figure 12. Observed Bouguer gravity field over Teague (Australia; Table 1); contour interval 10 μm s^{-2}. The outline of the rim of the structure is indicated by a circle. Note the interference with regional trends, and the presence of a gravity low over the structure.

to levels below the original crater floor. For example, in highly eroded large complex structures, only the central gravity high (see below) remains and the structure is characterised by only a positive anomaly — e.g., Connolly (Australia; Table 1; Shoemaker et al. 1989).

In general, simple craters and small complex craters (D <10 km) are characterised by a circular bowl-shaped residual negative anomaly — e.g., Wolfe Creek (Fudali 1979). For larger complex craters, the residual gravity low may be modified by the presence of a central gravity high, which is due to deeper denser crustal material being brought to the surface — e.g., Vredefort (Stepto 1990). The compressive regime in the central uplift of complex craters may also contribute to the central gravity high, through reduction in the initial impact-induced porosity (Grieve 1988). For larger structures (D >30 km) the maximum negative gravity anomaly reaches a limiting value of ~300 μm s^{-2} (Fig. 13).[1] This limit can be interpreted in terms of

Table 3. Geophysical signatures of terrestrial impact structures

	Simple	*Complex*
Gravity	Concentric low.	Concentric low. Central gravity high possible for D <30 km, probable for D >30 km. Central high <0.5D in diameter.
Magnetics	Simple low or subdued zone.	Simple low or subdued zone for D <10 km. Short-wavelength central anomalies possible for D = 10–40 km, probable for D >40 km. Central anomalies, generally, more localised than central gravity high.
Seismic	Low-velocity zone extending to ~>D.	Low-velocity zone coincident with structure. Possible high-velocity core for larger D. Zone of incoherent reflectors in target rocks at centre of structure and extending out to ~<0.5D; coherency increases with radial distance. Isotropic seismic zone corresponding to allochthonous deposits.
Electrical	Low-resistivity zone coincident with low-seismic-velocity zone.	Low-resistivity zone. Higher resistivities possible in central uplift of largest structures.

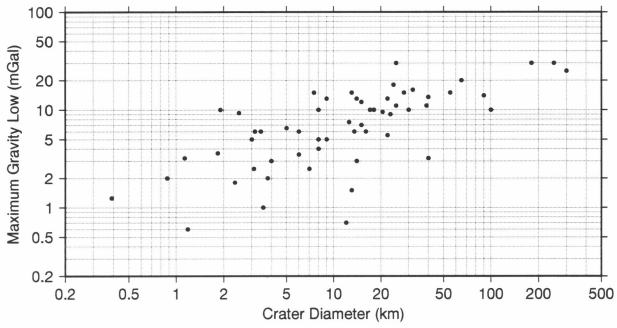

Figure 13. Maximum residual Bouguer gravity low relative to diameter for 58 terrestrial impact structures. Note the general trend of increasing gravity low with increasing diameter, until maximum values of ~300 μm s^{-2} are reached. Some of the scatter in the data is due to secondary effects, such as erosional level.

a maximum depth of fracturing associated with the structure (Basilevsky et al. 1983). For a density contrast of 0.1 t m^{-3} (100 kg m^{-3}), this corresponds to a depth of 8 km, below which it is expected that open fractures are essentially closed by lithostatic pressure (Perrier & Quiblier 1974).

Modelling of residual gravity data at simple craters (e.g., Fudali & Cassidy 1972; Grieve et al. 1989) shows that the apparent and true crater depths, d_a and d_t, are good estimates for model body dimensions, if the appropriate density contrasts are used. Hence, reduced densities due to extensive fracturing of autochthonous rocks beneath the crater floor do not appear to contribute significantly to the gravity anomaly at simple craters. In contrast, at complex structures, Pilkington & Grieve (1992) showed that the amount of stratigraphic uplift (SU) provides a useful estimate of the depth of the fractured zone, although, for D >30 km, this depth reaches a limiting value, as noted earlier, and the gravity effect is essentially constant.

Magnetic signature

Magnetic anomalies associated with terrestrial impact structures are generally more complex than associated gravity anomalies, and reflect the greater variation possible in the magnetic properties of rocks. The dominant effect at impact structures, however, is a magnetic low or subdued zone (Fig. 14; Dabizha & Fedynsky 1975; Clark 1983), which is commonly manifested as a truncation of the regional magnetic fabric. At larger structures, the magnetic low can be modified by the presence of shorter-wavelength large-amplitude localised anomalies which usually occur at or near the centre of the structure. These are generally small in areal extent, much less than that of the central gravity high, if present. Like the gravity signature, the magnetic signature does not reflect a one-to-one correspondence between the cross-sectional shape of the anomaly and the morphology of the impact structure. Furthermore, the existence of a central gravity high does not imply the presence of a central magnetic anomaly. Anomaly form, however, is somewhat dependent on the size of the structure: magnetic lows occur at small structures (D <10 km), and central high-amplitude anomalies at larger structures (D >40 km). There are also examples of structures with no obvious magnetic signature. For small impact structures in particular, aeromagnetic survey parameters may be inadequate to resolve the anomalous magnetic effects related to impact.

Magnetic anomalies related to impact may be caused by one or more of several mechanisms. Shock can serve to increase or decrease magnetisation levels. At peak pressures of ~1 GPa, shock demagnetisation can remove existing remanent magnetisation (e.g., Cisowski & Fuller 1978), and, at pressures of >10 GPa, magnetic susceptibility levels can be reduced. As well as a reduction in magnetisation levels, target rocks can also acquire a shock remanent magnetisation (SRM) in the direction of the Earth's field at the time of impact. The strength of SRM increases with ambient field intensity, and decreases with distance from the point of impact (Cisowski & Fuller 1978). SRM is most likely to occur in autochthonous target rocks that experience pressures >1 GPa and temperatures less than the Curie points of the magnetic phases present. Changes in magnetic properties due to mineralogical changes, particularly in mafic silicates, can occur at greater pressures (>30 GPa) — e.g., the production of magnetite from the thermal decomposition of amphibole and biotite (Fel'dman 1994). Similar effects can occur with ore minerals. For example, at lower pressures, titanomagnetite can result from the breakdown of ilmenite (Chao 1968).

As impact-melt rocks cool, they can acquire a thermoremanent magnetisation (TRM) in the direction of the Earth's magnetic field at the time of impact. This effect has led to several palaeomagnetic dating studies based on samples of impact-melt rocks and breccia (e.g., Robertson 1967; Pohl & Soffel 1971). A stable remanence and low directional scatter appear to be characteristics of palaeomagnetic data from impact-melt rocks, and reflect the rapid acquisition of the magnetisation (Pohl & Soffel 1971). Whole-rock melting can also result in the production of non-magnetic impact glasses (Pohl 1971).

The production of new magnetic phases resulting from elevated residual temperatures and hydrothermal alteration following impact may lead to the acquisition of a chemical remanent magnetisation (CRM) in the direction of the ambient field. The central magnetic anomaly at Saint Martin (Canada; Table 1) is attributed to the formation of hematite from the alteration of mafic silicates in the floor of the central uplift (Coles & Clark 1982). Residual post-impact heat and fracturing of the target rocks often result in the establishment of a local hydrothermal system, and the presence of oxygen favours higher magnetisation intensities. Post-impact processes — such as chemical weathering, leaching, and metamorphism — will further modify magnetic properties over longer time intervals.

Magnetisations have been observed in several different carriers — e.g., magnetite, hematite–ilmenite, and pyrrhotite. As expected, no one magnetic phase is characteristic of impact sites. Breccias and impact melt-rocks are characterised by Königsberger ratios (remanent/induced magnetisation) much larger than unity, so that induced magnetisation can be considered negligible, and observed magnetic anomalies are primarily due to remanent magnetisation levels. Several different sources producing the central magnetic anomalies are found at larger structures. At highly eroded structures (Vredefort), magnetic basement can be exposed in the central uplift. Anomalies can correspond to alteration zones within the central uplift area (Saint Martin), or the central anomaly can be caused by highly magnetic impact-melt rocks (Dellen, Sweden; Table 1) or suevite breccias (Ries).

[1] 1 μm s^{-2} = 1 g.u. = 0.1 mGal.

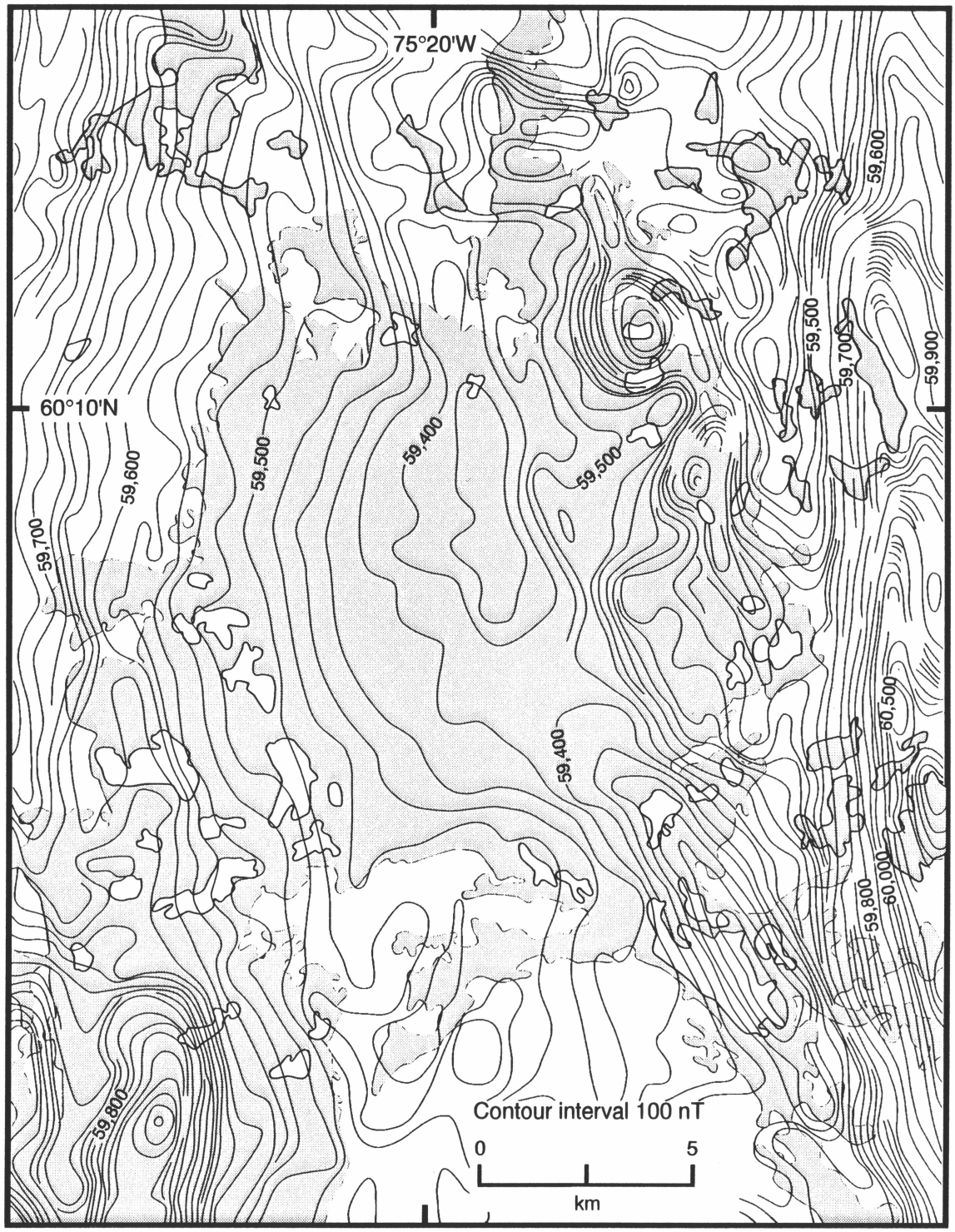

Figure 14. Observed magnetic field intensity over Couture (Canada; Table 1). Contour interval is 100 nT. Note the presence of a magnetic low over the area (shaded) of the roughly circular lake (the impact structure), and the lack of short-wavelength anomalies characteristic of the regional field.

The causes of magnetic lows at impact structures are not clear. The impact process undoubtedly results in a reduction in the magnetisation intensity of the target material. For uneroded craters, post-impact sedimentary infill will tend to be non-magnetic and so contribute to the reduced field intensity. This does not, however, explain the low fields over heavily eroded structures. By analogy with the gravity signature, an important contribution to the magnetic field must come from the parautochthonous target rocks beneath the floor of the structure. Recent studies of drillcore from several Canadian structures indicate that all impact lithologies show a reduction in both induced and remanent magnetisation levels, but this is not sufficient to produce all of the observed magnetic lows (Scott et al. 1995). The fractured target rocks also show diminished magnetisation levels at depths well below the floor, suggesting that the propagating shock wave is the likely cause.

Seismic signature

Seismic reflection and refraction data provide complementary information to potential-field data and geological observations on the characteristics of terrestrial impact structures. Reflection surveys allow for detailed imaging of the crater morphology, and for delineating seismically isotropic zones and incoherent reflections that are characteristic of brecciation and fracturing (e.g., at Tookoonooka; Gorter et al. 1989). The disturbance of coherent subsurface reflectors is most prominent in the central uplift of complex structures and decreases outward and downward from this zone (Brenan et al. 1975). As well as providing estimates of such morphological parameters as the dimensions of the central uplift, annular trough, and faulted blocks at the structural rim of complex structures, the depths to horizontal reflectors below the crater floor can be used to determine the amount of stratigraphic uplift (Fig. 2; Brown 1973).

The radial variation in impact-induced effects is also apparent on reflection seismic profiles. Where the transition between incoherent and coherent reflectors can be located, this provides an estimate of the dimensions of the so-called transient cavity (Melosh 1989; Juhlin & Pedersen 1987). The spatial density and penetration of faults decreases outwards from the annular trough at complex structures (Scott & Hajnal 1988). Towards the rim of complex structures, the moderately undeformed reflectors within downfaulted blocks allow such displacements to be mapped accurately (Brenan et al. 1975). As expected, the overall structural character of complex impact structures mapped by reflection seismic images corresponds to surface observations at exposed impact structures.

Refraction seismic surveys have proved useful for mapping the velocity distribution within terrestrial impact structures — specifically, zones of reduced velocities caused by fracturing and brecciation. At simple structures, velocity reductions of up to 50 per cent have been measured within the allochthonous breccia lens and sedimentary infill (Millman et al. 1960; Ackerman et al. 1975). In addition, at Barringer, the mapped lower-velocity zone also extends out beyond the rim of the structure. At complex structures, the low-velocity zone may extend well below the crater floor — e.g., at Ries (Pohl et al. 1977) — yet the uplift of deeper crustal material can lead to increased velocities, such as those occurring at Vredefort (Green & Chetty 1990).

Other signatures

As yet, electrical methods have been used little in the study of impact structures. The presence of fluids, however, in impact-induced fractures and pore spaces leads to decreased resistivity levels that can be mapped effectively by various methods. At the simple West Hawk structure, resistivities increase to 300 Wm at the crater rim, then up to ~800 Wm at one crater radius beyond the rim (Clark 1980). Studies within complex structures in crystalline targets have shown significant resistivity lows occurring within and extending out from the structural rim (Vishnevsky & Lagutenko 1986). At Siljan (Sweden; Table 1), Henkel (1992) has also mapped an increase in resistivity coinciding with the central uplift. Deeper investigations using magnetotelluric methods have not proved as informative, though low-resistivity zones have been mapped near several complex structures (e.g., Zhang et al. 1988; Mareschal & Chouteau 1990; Masero et al. 1994).

Summary and concluding remarks

We have attempted to summarise the basic signatures of terrestrial impact structures in Tables 2 and 3; by necessity, they represent a generalisation. Although local target rock geology has some importance, it tends to play only a second-order role in the character of terrestrial impact structures. Erosion is an important factor in the nature of the terrestrial impact record; it modifies the appearance of impact structures, even to the point of producing positive topographic features, and ultimately removes them from the record. Although it is probably premature to state that most of the obvious impact structures on the Earth's land surface have been discovered, some recent discoveries have resulted from the occurrence or re-examination of unusual lithologies rather than an obvious circular geological or topographic feature. For example, the breccias at Gardnos (Norway; Table 1) and Lockne (Sweden; Table 1) had been known for some time, but their shock-metamorphic effects were documented only recently, and they are now associated with the remnants of impact structures (Dons & Naterstad 1992; Lindström & Sturkell 1992; Therriault & Lindström 1995).

The occurrence of shock-metamorphic effects in association with some of the signature elements (Tables 2 and 3) provides the confirmatory evidence for an impact origin for somewhat enigmatic circular or quasicircular features at or near the Earth's surface. Several enigmatic structures bear some of the characteristics listed in Tables 2 and 3, but an impact origin remains to be confirmed for them through the documentation of shock-metamorphic features. One such feature is the Mount Toondina structure (Australia), which consists of a quasicircular 4-km-diameter central uplift; a report of the presence of shatter cones (E.M. Shoemaker, USGS, personal communication 1995) favours the prospect of Mount Toondina joining the growing list of confirmed terrestrial impact structures.

Terrestrial impact structures represent unusual geological events and, as such, they have resulted in local anomalous geological environments, some of which have produced significant economic deposits. About 25 per cent of known terrestrial impact structures have some form of economic deposit associated with them, and about half of these are currently exploited or have been exploited in the recent past. They range from local and now uneconomic (e.g., reserves of 300 000 t of hydrothermal Pb–Zn ores at Siljan) to world class (e.g., reserves of 1.6×10^9 t Ni–Cu–PGE ores at Sudbury). They also include hydrocarbon deposits (e.g., reserves of 50 million barrels of oil and 60 billion cubic feet of gas at Ames, USA; Table 1). The Ames impact structure not only produced the structural trap but also provided the source rocks, which are locally developed post-impact oil shales (Grieve 1996b). In addition, production includes hydrocarbons from non-traditional sources, such as the fractured crystalline rocks of the central uplift at Ames.

All currently known commercial hydrocarbon-producing impact structures and impact lithologies are located in North and Central America. There is, however, potential elsewhere. For example, the 55-km-diameter Tookoonooka structure has a zone of potential stratigraphic traps. Perhaps more importantly for hydrocarbon exploration, the Tookoonooka structure has created a shadow zone for hydrocarbon migration from the Eromanga Basin depocentre since the Early Cretaceous (Gorter et al. 1989). The early recognition of a hydrocarbon-prospective subsurface structure as an impact structure, with its moderately

invariant characteristics and potential for non-traditional sources, would significantly affect exploration strategies.

The level of knowledge concerning individual terrestrial impact structures is highly variable. The details for some are limited to the original discovery publication. As impact is such an important planetary geological process, and terrestrial impact craters are currently the only source of ground-truth data on large-scale impact events, this disregard is somewhat distressing. It is compensated, to some degree, by the fact that impact structures with similar dimensions and target rocks have the same major characteristics. Nevertheless, there is still much to be learnt about impact processes from terrestrial impact structures, particularly with respect to the third dimension. This is the property that is unobtainable from impact structures on other bodies in the solar system, and must be studied by remote-sensing methodologies.

Although the study of terrestrial impact structures has important ramifications for understanding impact processes, their study is not entirely an academic pursuit. The documentation of the terrestrial impact record provides a direct measure of the cratering rate on Earth (Grieve 1984), and thus a constraint on the hazard that impact presents to human civilisation (Gehrels 1994). The KT impact may have resulted in the demise of the dinosaurs as the dominant land-life form, and thus permitted the ascendency of mammals and, ultimately, humans. It is an inevitable fact, however, that if human civilisation persists into geological timescales it too will be subjected to a major impact-induced environmental crisis of immense proportions.

Acknowledgments

We thank M. Ford, J. Rupert, and J. Smith for their assistance in manuscript preparation. C. Tarlowski kindly provided the gravity data displayed in Figure 12. We gratefully acknowledge reviews by A. Hildebrand and A. Therriault.

References

Ackermann, H.D., Godson, R.H. & Watkins, J.S., 1975. A seismic refraction technique used for subsurface investigations at Meteor Crater, Arizona. Journal of Geophysical Research, 80, 765–775.

Alvarez, L.W., Alvarez, W., Asaro, F. & Michel, H.V., 1980. Extraterrestrial cause for the Cretaceous–Tertiary extinction. Science, 208, 1095–1108.

Badjukov, D.D., Lobitzer, H. & Nazarov, M.A., 1987. Quartz grains with planar features in the Triassic–Jurassic boundary sediments from Northern Limestone Alps. Lunar and Planetary Science, XVIII, 38–39 (abstract).

Banholzer, G. & Hörz, F., 1979. Distribution and shock metamorphism of crystalline clasts in the continuous deposits of the Ries crater, Germany. Lunar and Planetary Science, X, 63–65 (abstract).

Basilevsky, A.T., Ivanov, B.A., Florensky, K.P., Yakovlev, O.I., Fel'dman, V.I., Granovsky, L.V. & Sadovsky, M.A., 1983. Impact craters on the moon and planets (in Russian). Nauk Press, Moscow.

Bice, D.M., Newton, C.R., McCauley, S., Reiners, P.W. & McRoberts, C.A., 1992. Shocked quartz at the Triassic–Jurassic boundary in Italy. Science, 255, 443–446.

Bohor, B.F., 1990. Shock-induced microdeformations in quartz and other mineralogical indications of an impact event at the Cretaceous–Tertiary boundary. Tectonophysics, 171, 359–372.

Bohor, B.F., Foord, E.E., Modreski, P.J. & Triplehorn, D.M., 1984. Mineralogic evidence for an impact event at the Cretaceous–Tertiary boundary. Science, 224, 867–869.

Bohor, B.F., Modreski, P.J. & Foord, E.E., 1987. Shocked quartz in the Cretaceous–Tertiary boundary clays: evidence for a global distribution. Science, 236, 705–709.

Boslough, M.B., Cygan, R.T. & Izett, G.A., 1995. NMR spectroscopy of quartz from the K/T boundary: shock-induced peak boundaries, dense glass and coesite. Lunar and Planetary Science, XXVI, 149–150 (abstract).

Brenan, R.L., Peterson, B.L. & Smith, H.J., 1975. The origin of Red Wing Creek Structure: McKenzie County, North Dakota. Wyoming Geological Association, Earth Science Bulletin 8, 1–41.

Brown, A.R., 1973. A detailed seismic study of Gosses Bluff, Northern Territory. Bureau of Mineral Resources, Australia, Report 163.

Bucher, W.L., 1963. Are cryptovolcanic structures due to meteoritic impact? Nature, 197, 1241–1245.

Carter, N.L., Officer, C.B. & Drake, C.L., 1990. Dynamic deformation of quartz and feldspar: clues to causes of some natural crises. Tectonophysics, 171, 373–391.

Chao, E.C.T., 1968. Pressure and temperature histories of impact metamorphosed rocks — based on petrographic observations. In: French, B.M. & Short, N.M. (editors), Shock metamorphism of natural materials. Mono Book Corp., Baltimore, 135–158.

Cintala, M.J. & Grieve, R.A.F., 1994. The effects of differential scaling of impact melt and crater dimensions on lunar and terrestrial craters: some examples. In: Dressler, B.O., Grieve, R.A.F. & Sharpton, V.L. (editors), Large meteorite impacts and planetary evolution. Geological Society of America, Special Paper 293, 51–59.

Cisowski, S.M. & Fuller, M., 1978. The effect of shock on the magnetism of terrestrial rocks. Journal of Geophysical Research, 83, 3441–3458.

Clark, J.F., 1980. Geomagnetic surveys at West Hawk Lake, Manitoba, Canada. Canadian Department of Energy, Mines and Resources, Earth Physics Branch, Geomagnetic Series, 20, 1–11.

Clark, J.F., 1983. Magnetic survey data at meteoritic impact sites in North America. Geomagnetic Service of Canada, Earth Physics Branch, Open File, 83–5, 1–32.

Coles, R.L. & Clark, J.F., 1982. Lake St. Martin impact structure, Manitoba, Canada: magnetic anomalies and magnetizations. Journal of Geophysical Research, 87, 7087–7095.

Dabizha, A.I. & Fedynsky, V.V., 1975. The Earth's "star wounds" and their diagnosis by geophysical methods (in Russian). Zamlya Vselennaya, 3, 56–64.

Dence, M.R., 1968. Shock zoning at Canadian craters: petrography and structural implications. In: French, B.M. & Short, N.M. (editors), Shock metamorphism of natural materials. Mono Book Corp., Baltimore, 169–184.

Dence, M.R., Grieve, R.A.F. & Robertson, P.B., 1977. Terrestrial impact structures: principal characteristics and energy considerations. In: Roddy, D.J., Pepin, R.O. & Merrill, R.B. (editors), Impact and explosion cratering. Pergamon Press, New York, 247–275.

Deutsch, A. & Grieve, R.A.F., 1994. The Sudbury structure: constraints on its genesis from lithoprobe results. Geophysical Research Letters, 21, 963–966.

Dietz, R.S., 1968. Shatter cones in cryptoexplosion structures. In: French, B.M. & Short, N.M. (editors), Shock metamor-

phism of natural materials. Mono Book Corp., Baltimore, 267–285.

Dobrzhinetskaya, L.F., Eide, E.A., Larsen, R.B., Sturt, B.A., Tronnes, R.G., Smith, D.C., Taylor, W.R. & Posukhova, T.V., 1995. Microdiamond in high-grade metamorphic rocks of the Western Gneiss region, Norway. Geology, 23, 597–600.

Dons, J.A. & Naterstad, J., 1992. The Gardnos impact structure, Norway. Meteoritics, 27, 215 (abstract).

Dressler, B.O., 1984. General geology of the Sudbury area. In: Pye, E.G., Naldrett, A.J. & Giblin, P.E. (editors), The geology and ore deposits of the Sudbury structure. Ministry of Natural Resources, Toronto, 57–82.

Engelhardt, W.v., 1990. Distribution, petrography and shock metamorphism of the ejecta of the Ries crater in Germany — a review. Tectonophysics, 171, 259–273.

Engelhardt, W.v. & Bertsch, W., 1969. Shock induced planar deformation structures in quartz from the Ries Crater, Germany. Contributions to Mineralogy and Petrology, 20, 203–234.

Engelhardt, W.v. & Graup, G., 1977. Shock metamorphism in crystalline rocks from the Nördlingen 1973 research drill hole (in German). Geologica Bavarica, 75, 255–271.

Faggart, B.E., Basu, A.R. & Tatsumoto, M., 1985. Origin of the Sudbury complex by meteoritic impact: neodymium isotopic evidence. Science, 230, 436–439.

Fel'dman, V.I., 1994. The conditions of shock metamorphism. In: Dressler, B.O., Grieve, R.A.F. & Sharpton, V.L. (editors), Large meteorite impacts and planetary evolution. Geological Society of America, Special Paper 293, 121–132.

French, B.M., 1990. 25 years of the impact–volcanic controversy: is there anything new under the sun or inside the Earth? EOS, 71, 411–414.

French, B.M. & Short, N.M. (editors), 1968. Shock metamorphism of natural materials. Mono Book Corp., Baltimore.

Fudali, R.F., 1979. Gravity investigation of Wolf Creek crater, Western Australia. Journal of Geology, 87, 55–67.

Fudali, R.F. & Cassidy, W.A., 1972. Gravity reconnaissance at three Mauritanian craters of explosive origin. Meteoritics, 7, 51–70.

Ganapathy, R., 1980. A major meteorite impact on the Earth 65 million years ago: evidence from the Cretaceous–Tertiary boundary clay. Science, 209, 921–923.

Gehrels, T. (editor), 1994. Hazards due to comets and asteroids. University of Arizona Press, Tucson.

Gorter, J.D., Gostin, V.A. & Plummer, P.S., 1989. The enigmatic sub-surface Tookoonooka complex in south-west Queensland: its impact origin and implications for hydrocarbon accumulations. In: O'Neil, B.J. (editor), The Cooper and Eromanga Basins, Australia. Proceedings of the Petroleum Exploration Society of Australia, the Society of Petroleum Engineers, and the Australian Society of Exploration Geophysicists (SA Branches), Adelaide, 441–456.

Gostin, V.A., Haines, P.W., Jenkins, R.J.F., Compston, W. & Williams, I.S., 1986. Impact ejecta horizon within late Precambrian shales, Adelaide Geosycline, South Australia. Science, 233, 198–200.

Gostin, V.A., Keays, R.R. & Wallace, M.W., 1989. Iridium anomaly from the Acraman impact ejecta horizon: impact can produce sedimentary iridium peaks. Nature, 340, 542–544.

Green, R.W. & Chetty, P., 1990. Seismic refraction studies in the basement of the Vredefort structure. Tectonophysics, 171, 105–113.

Grieve, R.A.F., 1978. The melt rocks at Brent crater, Ontario, Canada. Proceedings of the 9th Lunar and Planetary Science Conference, 2579–2608.

Grieve, R.A.F., 1984. The impact cratering rate in recent time. Proceedings of the 14th Lunar and Planetary Science Conference. Journal of Geophysical Research, Supplement, 89, B403–B408.

Grieve, R.A.F., 1988. The formation of large impact structures and constraints on the nature of Siljan. In: Bodén, A. & Eriksson, K.G. (editor), Deep drilling in crystalline bedrock. Springer–Verlag, New York, 1, 328–348.

Grieve, R.A.F., 1996a. Extraterrestrial impact events: the record in the rocks and the stratigraphic column. Palaeogeography, Palaeoclimatology and Palaeoecology (in press).

Grieve, R.A.F., 1996b. Terrestrial impact structures: basic characteristics and economic significance, with emphasis on hydrocarbon production. Proceedings of the Ames Workshop, Oklahoma Geological Survey, Special Paper (in press).

Grieve, R.A.F., Dence, M.R. & Robertson, P.B., 1977. Cratering processes: as interpreted from the occurrence of impact melts. In: Roddy, D.J., Pepin, R.O. & Merrill, R.B. (editors), Impact and explosion cratering. Pergamon Press, New York, 791–814.

Grieve, R.A.F., Garvin, J.B., Coderre, J.M. & Rupert, J., 1989. Test of a geometric model for the modification stage of simple impact crater development. Meteoritics, 24, 83–88.

Grieve, R.A.F., Langenhorst, F. & Stöffler, D., 1996. Shock metamorphism of quartz in nature and experiment: II. Significance in geoscience. Meteoritics (in press).

Grieve, R.A.F. & Masaitis, V.L., 1994. The economic potential of terrestrial impact craters. International Geology Review, 36, 105–151.

Grieve, R.A.F. & Pesonen, L.J., 1992. The terrestrial impact cratering record. Tectonophysics, 216, 1–30.

Grieve, R.A.F., Robertson, P.B. & Dence, M.R., 1981. Constraints on the formation of ring impact structures, based on terrestrial data. In: Schultz, P.H. & Merrill, R.B. (editors). Multi-ring basins. Pergamon Press, New York, 37–57.

Grieve, R., Rupert, J., Smith, J. & Therriault, A., 1995. The record of terrestrial cratering. GSA Today, 5, 189, 194–196.

Grieve, R.A.F., Stöffler, D. & Deutsch, A., 1991. The Sudbury structure: controversial or misunderstood? Journal of Geophysical Research, 96, 22753–22764.

Grieve, R.A.F. & Therriault, A.M., 1995. Planar deformation features in quartz: target effects. Lunar and Planetary Science, XXVI, 515–516 (abstract).

Gudlaugsson, S.T., 1993. Large impact crater in the Barents Sea. Geology, 21, 291–294.

Gurov, E.P. & Gurova, E.P., 1991. Geological structure and composition of rocks in impact craters (in Russian). Nauk Press, Kiev.

Hanss, R.E., Montague, B.R., Davis, M.K., Galindo, C. & Hörz, G., 1978. X-ray diffractometer studies of shocked materials. Proceedings of the 9th Lunar and Planetary Science Conference, 2773–2787.

Hartmann, W., 1995. Planetary cratering: I. Lunar highlands and tests of hypotheses on crater populations. Meteoritics, 30, 451–467.

Hartmann, W.K. & Wood, C.A., 1971. Moon: origin and evolution of multi-ring basins. The Moon, 3, 3–78.

Henkel, H., 1992. Geophysical aspects of meteorite impact craters in eroded shield environment, with special emphasis on electric resistivity. Tectonophysics, 216, 63–90.

Hildebrand, A.R., Penfield, G.T., Kring, D.A., Pilkington, M., Camargo, A.Z., Jacobsen, S.B. & Boynton, W.V., 1991. Chicxulub crater: a possible Cretaceous/Tertiary boundary impact crater on the Yucatan Peninsula, Mexico. Geology, 19, 867–871.

Hildebrand, A.R., Pilkington, M., Connors, M., Ortiz-Aleman, C. & Chavez, R.E., 1995. Size and structure of the Chicxulub crater revealed by horizontal gravity gradients and cenotes. Nature, 376, 415–417.

Hörz, F., 1968. Statistical measurements of deformation structures and refractive indices in experimentally shock loaded quartz. In: French, B.M. & Short, N.M. (editors), Shock metamorphism of natural materials. Mono Book Corp., Baltimore, 243–253.

Hörz, F. & Quaide, W.L., 1973. Debye–Scherrer investigations of experimentally shocked silicates. The Moon, 6, 45–82.

Ivanov, B.A., 1994. Geochemical models of impact cratering: Puchezh–Katunki structure. In: Dressler, B.O., Grieve, R.A.F. & Sharpton, V.L. (editors), Large meteorite impacts and planetary evolution. Geological Society of America, Special Paper 293, 81–91.

Jahn, B., Floran, R.J. & Simonds, C.H., 1978. Rb–Sr isochron age of the Manicouagan melt sheet, Quebec, Canada. Journal of Geophysical Research, 83, 2799–2803.

Juhlin, C. & Pedersen, L.B., 1987. Reflection seismic investigations of the Siljan impact structure, Sweden. Journal of Geophysical Research, 92, 14113–14122.

Kieffer, S.W., 1971. Shock metamorphism of the Coconino Sandstone at Meteor Crater, Arizona. Journal of Geophysical Research, 76, 5449–5473.

Kieffer, S.W., Phakey, P.P. & Christie, J.M., 1976. Shock processes in porous quartzite: transmission electron microscope observations and theory. Contributions to Mineralogy and Petrology, 59, 41–93.

Kieffer, S.W. & Simonds, C.H., 1980. The role of volatiles and lithology in the impact cratering process. Reviews of Geophysics and Space Physics, 18, 143–181.

Koeberl, C., 1994. Tektite origin by hypervelocity asteroidal or cometary impact: target rocks, source craters, and mechanisms. In: Dressler, B.O., Grieve, R.A.F. & Sharpton, V.L. (editors), Large meteorite impacts and planetary evolution. Geological Society of America, Special Paper 293, 133–152.

Koeberl, C., Shirey, S.B. & Reimold, W.U., 1994. Re–Os isotope systematics as a diagnostic tool for the study of impact craters. In: New developments regarding the K/T event and other catastrophes in early Earth history. LPI Contribution 825, Lunar and Planetary Institute, Houston, 61–63 (abstract).

Lambert, P., 1981. Breccia dikes: geological constraints on the formation of complex craters. In: Schultz, P.H. & Merrill, R.B. (editors), Multi-ring basins. Pergamon Press, New York, 59–78.

Lange, M.A. & Ahrens, T.J., 1986. Shock-induced CO_2 loss from $CaCO_3$: implications for early planetary atmospheres. Earth and Planetary Science Letters, 77, 409–418.

Langenhorst, F. & Clymer, A., 1995. TEM examination of quartz from Massignano (Ancona, Italy). 4th International Workshop of the ESF Network on Impact Cratering and Evolution of Planet Earth, 107–108 (abstract).

Lindström, M. & Sturkell, E.F.F., 1992. Geology of the early Palaeozoic Lockne impact structure, central Sweden. Tectonophysics, 216, 169–185.

Loper, F.E. & McCartney, K., 1988. Shocked quartz found at the K/T boundary: a possible endogenous mechanism. EOS, 69, 961.

Mareschal, M. & Chouteau, M., 1990. A magnetotelluric investigation of the structural geology beneath Charlevoix Crater, Quebec. Physics of the Earth and Planetary Interiors, 60, 120–131.

Masaitis, V.L., Danilin, A.I., Mashchak, M.S., Raikhlin, A.I., Selivanovskaya, T.V. & Shadenkov, E.M., 1980. The geology of astroblemes (in Russian). Nedra Press, Leningrad.

Masaitis, V.L., Futergendler, S.I. & Gnevushev, M.A., 1972. Diamonds in impactites of the Popigai meteorite crater (in Russian). Zapiskio Vsesoyuznoge Mineralogicheskogo Obshchestva, 101, 108–112.

Masero, W., Schnegg, P.-A. & Fontes, S.L., 1994. A magnetotelluric investigation of the Araguainha impact structure in Mato Grosso–Goias, central Brazil. Geophysics Journal International, 116, 366–376.

McHone, J.F., Nieman, R.A., Lewis, C.F. & Yates, A.M., 1989. Stishovite at the Cretaceous–Tertiary boundary, Taton, New Mexico. Science, 243, 1182–1184.

Melosh, H.J., 1981. Atmospheric breakup of terrestrial impactors. In: Schultz, P.H. & Merrill, P.B. (editors), Multi-ring basins. Pergamon Press, New York, 29–35.

Melosh, H.J., 1989. Impact cratering: a geologic process. Oxford University Press, New York.

Millman, P.M., Liberty, B.A., Clark, J.F., Willmore, P. & Innes, M.J.S., 1960. The Brent crater. Ottawa Dominion Observatory, Publication 24, 1–43.

Milton, D.J., 1977. Shatter cones — an outstanding problem in shock mechanics. In: Roddy, D.J., Pepin, R.O. & Merrill, R.B. (editors), Impact and explosion cratering. Pergamon Press, New York, 703–714.

Milton, D.J., Glikson, A.Y. & Brett, R., 1996. Gosses Bluff — an end-Jurassic impact structure in central Australia. Part 1: geology. AGSO Journal of Australian Geology & Geophysics (this issue).

Officer, C.B., 1992. The relevance of iridium and microscopic dynamic deformation features toward understanding the Cretaceous/Tertiary transition. Terra Nova, 4, 394–404.

Palme, H., 1982. Identification of projectiles of large terrestrial impact craters and some implications for the interpretation of Ir-rich Cretaceous/Tertiary boundary layers. Geological Society of America, Special Paper 190, 223–233.

Palme, H., Goebel, E. & Grieve, R.A.F., 1979. The distribution of volatile and siderophile elements in the impact melt of East Clearwater (Quebec). Proceedings of the 10 th Lunar and Planetary Science Conference, 2465–2492.

Palme, H., Grieve, R.A.F. & Wolf, R., 1981. Identification of the projectile at Brent crater, and further considerations of projectile types at terrestrial craters. Geochimica et Cosmochimica Acta, 45, 2417–2424.

Perrier, R. & Quiblier, J., 1974. Thickness changes in sedimentary layers during compaction history: methods for quantitative evaluation. American Association of Petroleum Geologists, Bulletin 58, 507–528.

Pevzner, L.A., Kirjakov, A.F., Vorontsov, A.K., Masaitis, V.L., Mashchak, M.S. & Ivanov, B.A., 1992. Vorotilovskaya drillhole: first deep drilling in the central uplift of a large terrestrial impact crater. Lunar and Planetary Science, XXII, 1063–1064 (abstract).

Pike, R.J., 1977. Size-dependence in the shape of fresh impact craters on the moon. In: Roddy, D.J., Pepin, R.O. & Merrill, R.B. (editors), Impact and explosion cratering. Pergamon Press, New York, 489–509.

Pike, R.J., 1985. Some morphologic systematics of complex impact structures. Meteoritics, 20, 49–68.

Pilkington, M. & Grieve, R.A.F., 1992. The geophysical signature of terrestrial impact craters. Reviews of Geophysics, 30, 161–181.

Poag, C.W., Powars, D.S., Poppe, L.J. & Mixon, R.B., 1994. Meteoroid mayhem in Ole Virginny: source of the North American tektite strewn field. Geology, 22, 691–694.

Pohl, J., 1971. On the origin of the magnetization of impact breccias on Earth. Zeitschrift für Geophysik, 37, 549–555.

Pohl, J. & Soffel, H., 1971. Paleomagnetic age determination of the Rochechouart impact structure (France). Zeitschrift für Geophysik, 37, 857–866.

Pohl, J., Stöffler, D., Gall, H. & Ernston, K., 1977. The Ries impact crater. In: Roddy, D.J., Pepin, R.O. & Merrill, R.B. (editors), Impact and explosion cratering. Pergamon Press, New York, 343–404.

Redeker, H.J. & Stöffler, D., 1988. The allochthonous polymict breccia layer of the Haughton impact crater, Devon Island, Canada. Meteoritics, 23, 185–196.

Reimold, W.U. & Colliston, W.P., 1994. Pseudotachylites of the Vredefort Dome and the surrounding Witwatersrand Basin, South Africa. Geological Society of America, Special Paper 293, 177–196.

Robertson, P.B., 1980. Anomalous development of planar deformation features in shocked quartz of porous lithologies. Lunar and Planetary Science, XI, 938–940 (abstract).

Robertson, P.B. & Grieve, R.A.F., 1977. Shock attenuation at terrestrial impact structures. In: Roddy, D.J., Pepin, R.O. and Merrill, R.B. (editors), Impact and explosion cratering. Pergamon Press, New York, 687–702.

Robertson, W.A., 1967. Manicouagan, Quebec, paleomagnetic results. Canadian Journal of Earth Sciences, 4, 641–649.

Roddy, D.J., Pepin, R.O. & Merrill, R.B. (editors), 1977. Impact and explosion cratering. Pergamon Press, New York.

Sazonova, L.V., 1981. Planar deformations in quartz from authigenic breccia from the central uplift of the Kara meteorite crater (in Russian). Doklady Akadamii Nauk SSSR, 261, 731–734.

Sazonova, L.V., Karotayeva, N.N., Ponomarev, G.Y. & Dabizha, A.I., 1981. The Kara meteorite crater (in Russian). In: Marakusheva, A.A. (editor), Impactites. Moscow State University Press, Moscow, 93–135.

Schneider, W., 1971. Petrologic study of the Bunte breccia at the Nördlingen Ries (in German). Neues Jahrbuch für Mineralogie, Abhandlungen, 114, 136–174.

Scott, D. & Hajnal, Z., 1988. Seismic signature of the Haughton structure. Meteoritics, 23, 239–247.

Scott, R.G., Pilkington, M., Tanczyk, E.I. & Grieve, R.A.F., 1995. Magnetic properties of three impact structures in Canada. Meteoritics, 30, 576–577 (abstract).

Sharpton, V.L., Burke, K., Camargo-Zanoguera, A., Hall, S.A., Lee, D.S., Marin, L.E., Suarez-Reynoso, G., Quezada-Muneton, J.M., Spudis, P.D. & Urrutia-Fucugauchi, J., 1993. Chicxulub multiring impact basin: size and other characteristics derived from gravity analysis. Science, 261, 1564–1567.

Shoemaker, E.M., Shoemaker, C.S. & Plescia, J.B., 1989. Gravity investigation of the Connolly basin impact structure, Western Australia. Lunar and Planetary Science, XX, 1010–1011 (abstract).

Short, N.M., 1970. Anatomy of a meteorite impact crater: West Hawk Lake, Manitoba, Canada. Geological Society of America, Bulletin 81, 609–648.

Smit, J. & Hertogen, J., 1980. An extraterrestrial event at the Cretaceous–Tertiary boundary. Nature, 285, 158–200.

Spray, J.G. & Thompson, L.M., 1995. Friction melt distribution in terrestrial multi-ring impact basins. Nature, 373, 130–132.

Stepto, D., 1990. The geology and gravity field in the central core of the Vredefort structure. Tectonophysics, 171, 75–103.

Stöffler, D., 1971. Progressive metamorphism and classification of shocked and brecciated crystalline rocks in impact craters. Journal of Geophysical Research, 76, 5541–5551.

Stöffler, D., 1972. Deformation and transformation of rock-forming minerals by natural and experimental shock processes: I. Behavior of minerals under shock compression. Förtschritte der Mineralogie, 49, 50–113.

Stöffler, D., 1974. Deformation and transformation of rock-forming minerals by natural and experimental shock processes: II. Physical properties of shocked minerals. Förtschritte der Mineralogie, 51, 256–289.

Stöffler, D., 1984. Glasses formed by hypervelocity impact. Journal of Non-Crystalline Solids, 67, 465–502.

Stöffler, D., Bischoff, L., Oskierski, W. & Wiest, B., 1988. Structural deformation, breccia formation, and shock metamorphism in the basement of complex terrestrial impact craters: implications for the cratering process. In: Bodén, A. & Eriksson, K.G. (editors), Deep drilling in crystalline bedrock. Springer–Verlag, New York, 1, 277–297.

Stöffler, D., Deutsch, A., Avermann, M., Bischoff, L., Brockmeyer, P., Buhl, D., Lakomy, R. & Müller-Mohr, V., 1994. The formation of the Sudbury structure, Canada: towards a unified impact model. In: Dressler, B.O., Grieve, R.A.F. & Sharpton, V.L. (editors), Large meteorite impacts and planetary evolution. Geological Society of America, Special Paper 293, 303–318.

Stöffler, D., Ewald, U., Ostertag, R. & Reimold, W.U., 1977. Research drilling Nördlingen 1973, Ries: composition and texture of polymict impact breccias. Geologica Bavarica, 75, 163–190.

Stöffler, D. & Hornemann, U., 1972. Quartz and feldspar glasses produced by natural and experimental shock. Meteoritics, 7, 371–394.

Stöffler, D. & Langenhorst, F., 1994. Shock metamorphism of quartz in nature and experiment: 1. Basic observation and theory. Meteoritics, 29, 155–181.

Therriault, A.M., Grieve, R.A.F. & Reimold, W.U., 1995. How big is Vredefort? Meteoritics, 30, 586–587 (abstract).

Therriault, A.M. & Lindström, M., 1995. Planar deformation features in quartz grains from the resurge deposit of the Lockne structure, Sweden. Meteoritics, 30 (in press).

Therriault, A.M., Reid, A.M. & Reimold, W.U., 1993. Original size of the Vredefort structure, South Africa. Lunar and Planetary Science, XXIV, 1419–1420 (abstract).

Tingate, P.R., Lindsay, J.F. & Marshallsea, S.J., 1996. Impact structures as potential petroleum exploration targets: Gosses Bluff, a Late Jurassic example from central Australia. AGSO Journal of Australian Geology & Geophysics, this issue.

Vishnevsky, S.A. & Lagutenko, V.N., 1986. The Ragozinka astrobleme: an Eocene crater in the central Urals (in Russian). Doklady Akademii Nauk SSSR, 14, 1–42.

Wallace, M.A., Gostin, V.A. & Keays, R.R., 1990. Acraman impact ejecta and host shales: evidence for low-temperature mobilization of iridium and other platinoids. Geology, 18, 132–135.

Wallace, M.W., Gostin, V.A. & Keays, R.R., 1996. Sedimentology of the Neoproterozoic Acraman impact-ejecta horizon, South Australia. AGSO Journal of Australian Geology & Geophysics, this issue.

Wasson, J.T., 1991. Layered tektites: a multiple impact origin for the Australasian tektites. Earth and Planetary Science Letters, 102, 95–109.

Wolf, R., Woodrow, A.B. & Grieve, R.A.F., 1980. Meteoritic material at four Canadian impact craters. Geochimica et Cosmochimica Acta, 44, 1015–1022.

Wood, C.A. & Head, J.W., 1976. Comparison of impact basins on Mercury, Mars and the moon. Proceedings of the 7th Lunar Science Conference, 3629–3651.

Zhang, P., Rasmussen, T.M. & Pedersen, L.B., 1988. Electric resistivity structure of the Siljan impact region. Journal of Geophysical Research, 93, 6485–6501.